

Joint Centre for Mesoscale Meteorology, Reading, UK



A Meteorological Assessment of the Geostrophic
Co-ordinate Transform and Error Breeding System
when used in 3D Variational Data Assimilation.

Adrian Semple

Internal Report No. 130
NWP Technical Report No. 357

June 2001

Met Office Joint Centre for Mesoscale Meteorology Department of Meteorology
University of Reading PO Box 243 Reading RG6 6BB United Kingdom
Tel: +44 (0)118 931 8425 Fax: +44 (0)118 931 8791
www.metoffice.com



A Meteorological Assessment of the Geostrophic Co-ordinate Transform and Error Breeding System when used in 3D Variational Data Assimilation.

Adrian Semple

June 2001

Abstract

This report documents research carried out to assess the impact of two schemes (the Geostrophic co-ordinate Transform (GCT), and Errors of the Day (EotD)) aimed at improving the assimilation of observational data by 3D VAR. Impact of the GCT and EotD schemes are traced through the data analysis procedure by the combined use of pseudo single observation tests (SOTs) and extended operational trial data.

It has been found through the SOTs that both schemes interact with the existing assimilation system successfully and produce modifications to the way in which the observational information is assimilated in a meteorologically sound way. Further, modifications made to the analysis increments in 3DVAR survive through the change in grid and resolution to the UM.

Both schemes show successes in their design aims: the GCT is shown to introduce exceptional flow dependence in the vicinity of baroclinic zones and the EotD is shown to identify regions of the model which are rapidly growing and are consistent with what one would expect meteorologically. In addition, the EotD has also been seen to exhibit good flow dependence.

Each scheme has been assessed operationally on individual extra-tropical cyclone cases.

The GCT is observed to have a measurable impact on the UM analyses with modifications being made throughout the northern and southern hemisphere storm track regions. These impacts have been studied in detail by assessing the thermal structure within a region of maximum GCT modification and have been shown to amount to relatively small modifications to thermal gradient and position. In some cases, these impacts are observed to provide relatively small positive changes to forecast performance of mslp, although the overall impact is predominantly neutral. There is evidence in these case studies that suggest the GCT may have some positive effect on forecast precipitation rates.

Operationally, the EotD is observed to have a more consistent impact on UM analyses than the GCT, with more extensive and intense modifications, again concentrated within the northern and southern hemisphere storm track regions. In depth investigations relating operational observational data with the analysis increments output by VAR have shown that the EotD scheme is working correctly within its design. These modifications have been observed to have a significant positive impact in some cases of cyclogenesis. No significant negative impact has been observed.

It is suggested in this report that the observed relative performance of the GCT and EotD is perhaps what one would expect when one considers their specific roles. The GCT is not an initiative designed to improve poor analyses, but is better considered as a means of reducing the detrimental effect that VAR may have in regions of baroclinicity. In this respect therefore, one would not expect the GCT to have huge impacts on forecasts. The EotD however, is specifically designed to effect the operation of VAR in regions where the background field is inferred to be less reliable, and so one would expect a more noticeable impact on forecasts by the EotD scheme.

1. INTRODUCTION.....	4
1.1 TRIAL OVERVIEW.....	4
1.2 3D VAR SYSTEM OVERVIEW	5
2. ASSESSMENT OF THE GCT AND EBS USING PSEUDO SINGLE OBSERVATIONS TESTS	7
2.1 OVERALL COMPARISON (3D VAR, GCT, EOTD).....	7
2.2 SPECIFICS OF THE GCT	9
2.3 SPECIFICS OF THE EOTD.....	10
2.4 PROPAGATION OF GCT AND EBS EFFECTS IN DATA ANALYSIS	11
3. IMPACT ASSESSMENT OF THE GCT & EOTD ON INDIVIDUAL CYCLOGENESIS UM FORECASTS	15
3.1 IMPACT OF THE GCT AND EOTD ON OPERATIONAL VAR ANALYSES, AND THEIR EFFECT ON UM FORECASTS.....	15
3.2 GCT CASE STUDY BASED ON MAXIMUM ANALYSIS MODIFICATION, 12Z 21/12/99	17
3.2.1 Analysis Changes	17
3.2.2 Forecast Changes.....	20
3.2.3 Overall Assessment of the GCT in this Case Study	23
3.3 EOTD CASE STUDY BASED ON MAXIMUM ANALYSIS MODIFICATION, 12Z 21/12/99.....	24
3.3.1 Analysis Changes - Verification of the EotD Operation	24
3.3.2 Forecast Changes.....	26
3.3.3 Overall Assessment of the EotD in this Case Study.....	27
3.3.4 GCT Impact in the same region	28
4. BREDMODE ACTIVITY AND UM FORECAST PERFORMANCE	29
5. DISCUSSION & RECOMMENDATIONS.....	32
6. ACKNOWLEDGEMENTS.....	36

1. Introduction

The aim of the Geostrophic Co-ordinate Transform (GCT)¹ and Errors of the Day (EotD)² is to make better use of the existing observational network and existing data assimilation systems (3D Variational Data Assimilation, (3D VAR)) particularly in order to improve forecasts of extra-tropical cyclones in the North Atlantic region.

The 3D VAR scheme attributes a region of influence to an observation, in which the three-dimensional distribution associated with the observation is assumed to be isotropic. This means that the correlation between two points depends only on the magnitude of their separation and not on its direction. The isotropic assumption means that 3D VAR attributes the same distribution to the observation whether the observation is located near a frontal zone or not. The result is that any observation assimilated near a frontal zone may cause a weakening of the baroclinic region relative to reality through its representation in the VAR increment field (the output of VAR).

To remedy this, the GCT scheme aims to incorporate flow-dependence into the assimilation by allowing the distribution of the observation to be anisotropic on the VAR grid. This is achieved by transferring the data analysis into a geostrophic co-ordinate system which is not regular like the VAR grid but has a distortion determined by the geostrophic wind component on the (x,y) plane. The frontal discontinuity in the VAR co-ordinate system appears more regular in the distorted geostrophic co-ordinate system and thus violates the isotropic assumption less. Once analysed, the fields are then transformed back to the VAR grid.

The 3D VAR scheme requires knowledge of the background error correlations in order to produce the best analysis. Estimation of these errors is currently achieved by 24 hour and 48 hour forecast differences averaged over a two week period and so fails to give an indication of the daily variation in the magnitude and structure of the errors. The EotD scheme uses an Error Breeding System (EBS) and is being trialed as a route to better estimate the background 'Errors of the Day'. It provides the errors as three-dimensional 'bredmodes' which originate as forecast differences between low-resolution short-range forecasts run from perturbed analyses. Bredmodes represent regions of the model atmosphere which have grown rapidly in the preceding time period and so represent areas which are likely to be associated with the greatest background errors. Given a suitable bredmode structure, the EotD scheme allows the distribution of the observation within VAR to change according to the local bredmode structure, so that observational information can have a greater or lesser influence depending on the inferred local background error.

The aim of this report is to document research carried out in order to assess both the GCT and EotD schemes relative to 3D VAR. It aims to establish whether both schemes are (1) assimilating observations in a meteorologically sound way, (2) having a positive, negative or neutral impact on individual storm forecasts, and (3) make recommendations on whether the continued use of the schemes is appropriate.

1.1 Trial Overview

The assessment documented in this report is based on the following trials, all of which were ran at a horizontal resolution of 288 x 217 and a vertical resolution of 30 levels. The GCT trial ran from the 26th November to the 28th December 1999. The control run for the GCT

¹ For technical documentation the reader is referred to VSDP12 by Mark Dubal.

² For technical documentation the reader is referred to DADP5 and VSDP26 by Dale Barker.

trial (Cntrl00) initially ran from the 26th November to the 17th December 1999, but was later extended to the 28th December. The EBS trial (EBS01) ran from the 26th November to the 30th December 1999. However, as the error breeding cycle requires a minimum of two weeks 'spin-up' time, only events after the 10th December were considered. The control run for the EBS trial (Cntrl01) ran from the 26th November to the 30th December 1999.

Missing output files from these trials at various periods strongly limited the choice of suitable cases for study, particularly when intercomparisons between the trials were being made.

1.2 3D VAR System Overview

The use of the GCT and EBS with 3D VAR involves reconfigurations between various model grids and resolutions, and the sequential creation of error-bred, VAR and model fields.

Figure 1 shows a schematic of the systems involved. The figure specifically relates to Single Observation tests, but the general interaction between the systems is true for VAR working operationally and within the trials discussed in Section 1.1. At the top left-hand corner is a Unified Model (UM) analysis field at 432x325 resolution on the Arakawa-B Lorenz grid. 3D VAR requires its own background field (the 'Linearisation State', or 'LS' Dump) at half UM resolution (216x163) on the Arakawa-C Charney-Phillips grid. The creation of this is shown at the start of the red path on the diagram. A pseudo Single Observation Test (SOT) is performed in VAR using this field as the background field, where the observation is specified in the VAR job as some suitable increment. The output of the VAR job, the PF (Perturbation Forecast) Analysis consists of the increment fields which will be added by the IAU (Incremental Analysis Update) to the background field in order to initialise the UM (Unified Model). The PF analysis is on the VAR grid.

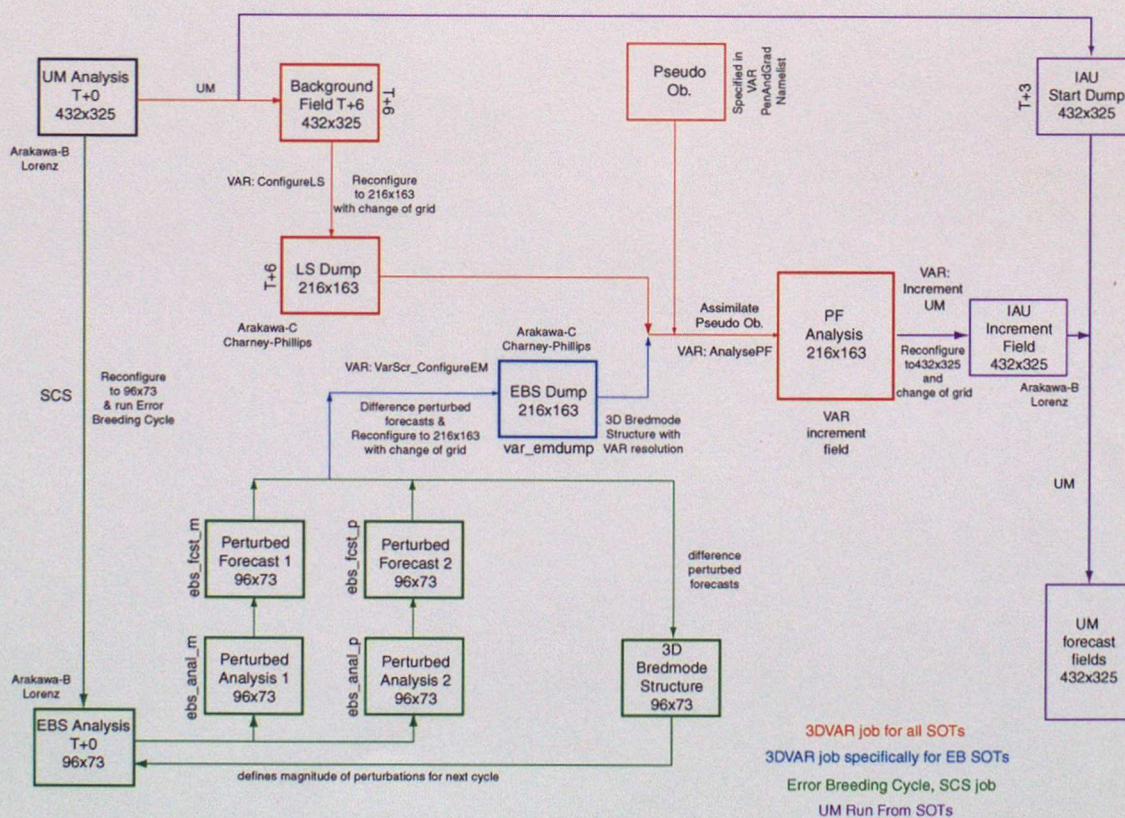


Figure 1 Schematic illustrating the coupling between 3D VAR and the EBS and GCT systems used in this assessment. Pseudo Single Observation Tests (SOTs) are discussed in Section 2. UM runs from SOT increment fields are discussed in Section 2.4.

Activating the GCT in these trials simply involves specifying the GCT within the AnalysePF VAR routine.

The use of the EBS is a little more involved. The EBS is run using the Suite Control System (SCS) for the period of the trials as indicated by the green path on the diagram. Although the EotD trial is run at 288 x 217 resolution, the error breeding cycle (producing the bredmode structures) are generated at the coarser resolution of 96 x 73, and remaining on the Arakawa-B Lorenz grid. The EBS generates perturbed forecast fields during its operation which are required for use in single observation tests. In normal operation these forecast fields are used within the EBS to generate the bredmode structures which are used within the error breeding system itself and for diagnostic purposes. Single observation tests for the EBS require the creation of an EBS dump. This is the bredmode structure of the EBS reconfigured to the VAR resolution (216x163) and Arakawa-C Charney-Phillips grid. The EBS dump is then used as an additional input field to the VAR AnalysePF job.

2. Assessment of the GCT and EBS Using Pseudo Single Observations Tests

2.1 Overall Comparison (3D VAR, GCT, EotD)

The aim of this section is to address the effectiveness of the GCT and EBS in the modification of the VAR analysis increments. For this purpose single observation tests were carried out at different positions in the model in relation to frontal zones and extra-tropical cyclones. Single Observation tests consist of assimilating a pseudo increment of a variable within the model atmosphere. The size of the increment chosen in these tests is of the order of magnitude that one would expect for real observations.

The pseudo single Observation Test discussed here consisted of a potential temperature increment of 1K (error of 1.7) on model level 11 (approximately 525hPa) at 47N 30W. At this time a strong baroclinic zone existed across the northern Atlantic Ocean, orientated east-west from Newfoundland to the UK. This provided an ideal case study in order to see how each system (VAR, GCT and EBS) behaved near frontal zones. Figure 2 shows the θ_1 PF analysis field on model level 11 for the VAR system, VAR with the GCT (VAR+GCT) and VAR with the EBS (VAR+EBS) (θ_1 is used as θ is unavailable in trial output). Also shown is the intensity distribution on this model level for the analysis increments for each scheme, illustrating the number of grid boxes with each increment value. Figure 3 shows cross sections through the line AB as indicated for each of the three schemes.

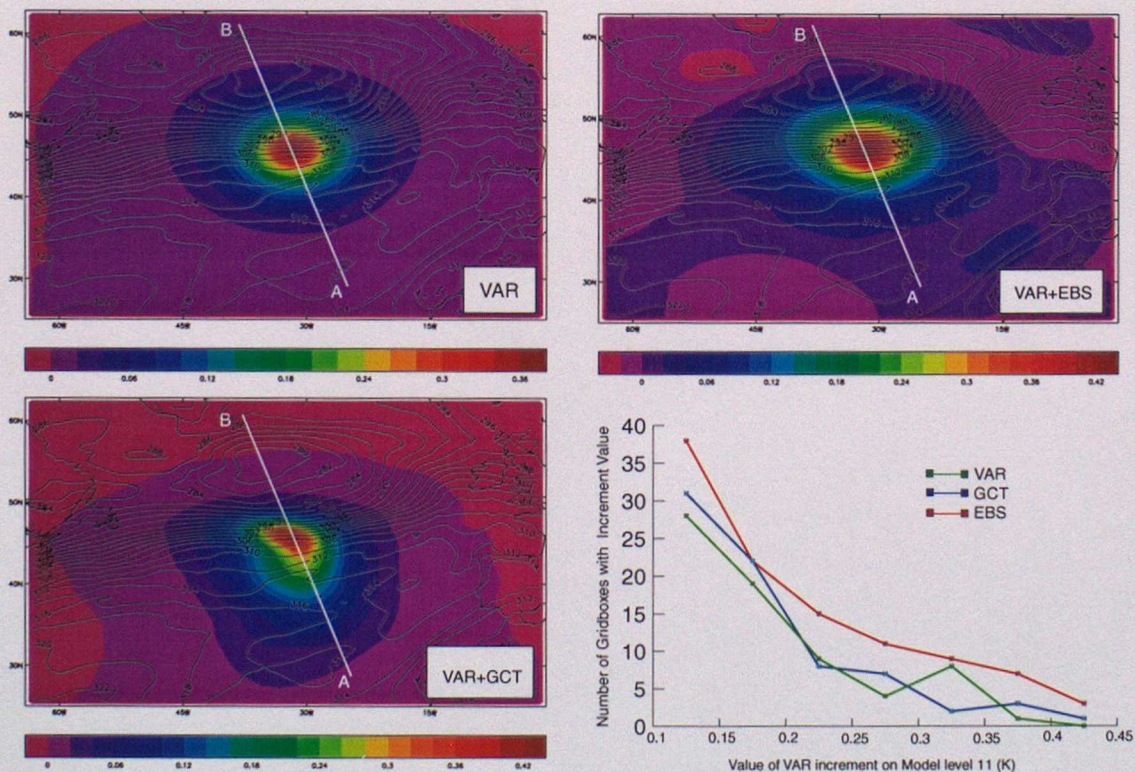


Figure 2 Single Observation tests (θ increment of 1, error 1.7, model level 11) for VAR, VAR+GCT and VAR+EBS near a frontal zone in the North Atlantic, 1200 UTC 24th December 1999. The coloured field shows the θ_1 analysis increments output by VAR in each case as a result of the single observation. The black contours show the UM θ_1 analysis on model level 11. The graph shows the intensity distribution of the analysis increments on model level 11 for each case.

As discussed earlier, the VAR scheme attributes a three-dimensional region of influence to the observation, in which the distribution associated with the observation is assumed to be isotropic. This can be seen by the distribution of the VAR single observation test in Figure 2 which represents its horizontal influence (although VAR attributes a purely spherical distribution, the pattern looks slightly oval due to the map projection). The isotropic assumption is clearly evident in the vertical also (Figure 3). The distribution of the observation is the same as though there were no frontal zone, and is largely spherical.

Although an increment of potential temperature was placed within the troposphere, the cross sections in Figure 3 indicate the presence of a region of cooling in the stratosphere, vertically above the increment. This is the sort of response that one would hope for within the assimilation system, as it is indicative of (geostrophic) balance information being propagated through the analysis by the background covariances. The wind and temperature fields that result from an incremental temperature perturbation are qualitatively consistent with those attributable to a potential vorticity anomaly located vertically between the temperature dipole³.

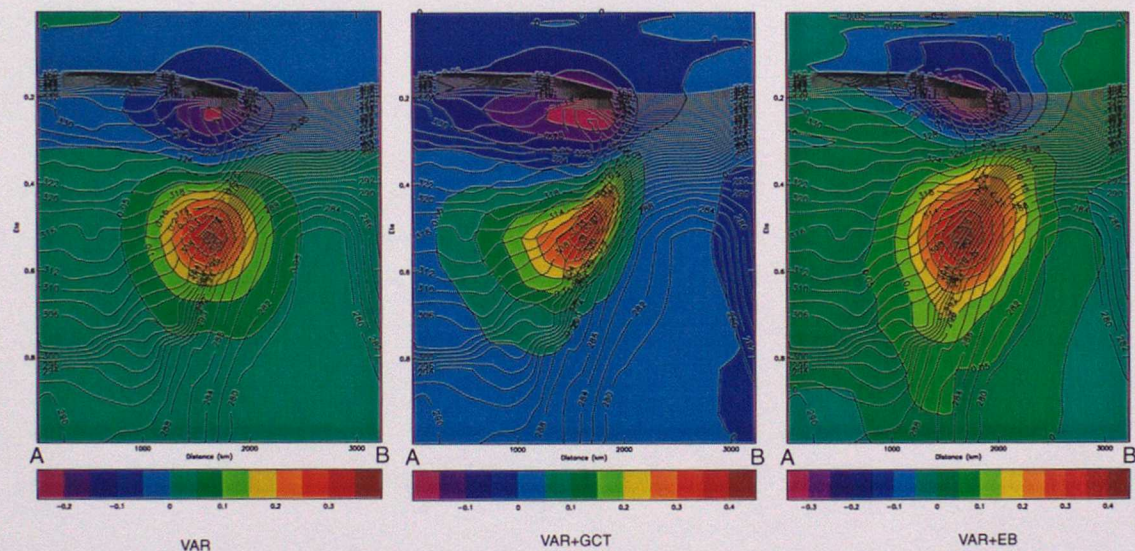


Figure 3 Cross sections (colour field) through AB shown in Figure 2 for VAR, VAR+GCT and VAR+EBs. Black contours show UM θ_1 analysis.

The effect of the GCT scheme is that the observation is no longer spread uniformly around the insertion point. For purposes of comparison, consider the point on Figure 2 at which the increment value on model level 11 drops to ~10% it's maximum value (dark blue). The distribution for the GCT scheme extends ~70% further into the warm air to the south than that with the VAR scheme. The extent to the north in the GCT is roughly halved relative to VAR, whereas the distribution along the front remains largely the same.

The graph on Figure 2 shows that the intensity distribution for the GCT is similar to that for VAR, although there appears to be a relative reduction in the higher value analysis increments (0.3 to 0.35) for the GCT and an increase of the GCT relative to VAR either side of this. This is evidence that the GCT is successfully redistributing the observational information rather than amplifying or attenuating it. In cross section the GCT has distorted the distribution so that it appears to flow up the frontal zone which may be seen on the right of the panel. This results in more of the increment being assimilated on the warm side of the front (i.e. the side of the front on which the observation has been placed), and is consistent with the distribution in Figure 2.

³ See 'Potential Vorticity and the Electrostatics Analogy: Quasi-Geostrophic Theory' by C Bishop and A J Thorpe, JCMM internal Report 19.

Figure 2 also shows that in this case the EBS has the effect of increasing the horizontal analysis increments along the frontal zone relative to VAR, whilst maintaining the meridional extent. In addition, the intensity profile for the EotD is approximately 50% larger than both the GCT and VAR schemes. This is a product of the bredmode intensity pattern shown in Figure 5, in which the observation increment pattern is superimposed upon the larger high intensity bredmode structure distribution, thus increasing the relative number of all increment values.

In this case, the EotD scheme therefore has had the effect of both boosting (by the number of gridboxes with higher increment values) and extending the horizontal observation influence along the frontal zone. In cross section (Figure 3), the VAR+EB analysis increments are elongated vertically along the baroclinic region with respect to the VAR analysis increments, and influence of the observation is seen at far lower levels in the troposphere than either the VAR or VAR+GCT cases. The cross section also shows that the increased intensity of the EBS analysis increments measured on model level 11 is true on all model levels relative to the VAR and GCT cases. All this behaviour is in accordance with that expected from the relevant bredmode and the design intentions of the EotD scheme.

2.2 Specifics of the GCT

The flow dependence introduced by the GCT into VAR is illustrated in more detail in Figure 4, which shows cross sections through single observation tests identical to that discussed above, and at the same analysis time, but in which the position of the observation has been varied meridionally.

The top left shows an assimilated observation in the warm air to the south of the strong baroclinic region. Here, the GCT has a small effect only in the periphery of the observation that comes into the vicinity of the baroclinic region. Otherwise, the distribution of the analysis increment is more similar to that one would expect with 3D VAR. As the observation is assimilated closer to the baroclinic region, the GCT plays a more major role in distorting the distribution so that the observation appears to flow up the frontal zone.

On the bottom left, the observation is located to the north of the baroclinic region and occupies a cold pool to the north. Here, the analysis increments lose much of the flow characteristics that were observed previously, but appear to be bounded within the cold pool by the baroclinicity to all sides. As the observation is assimilated further north, it occupies a weaker region of baroclinicity, which is responded to by the GCT by a corresponding weaker distortion, but in the opposite sense to that observed to the south. The spherical distribution of VAR then becomes more dominant as the observation is located to the north of the weaker baroclinic region, and the effect of the GCT diminishes.

The behaviour shown here exemplifies the desired effects of the GCT in the modification of the VAR analysis, and illustrates that the effect of the GCT on observations is meteorologically sound.

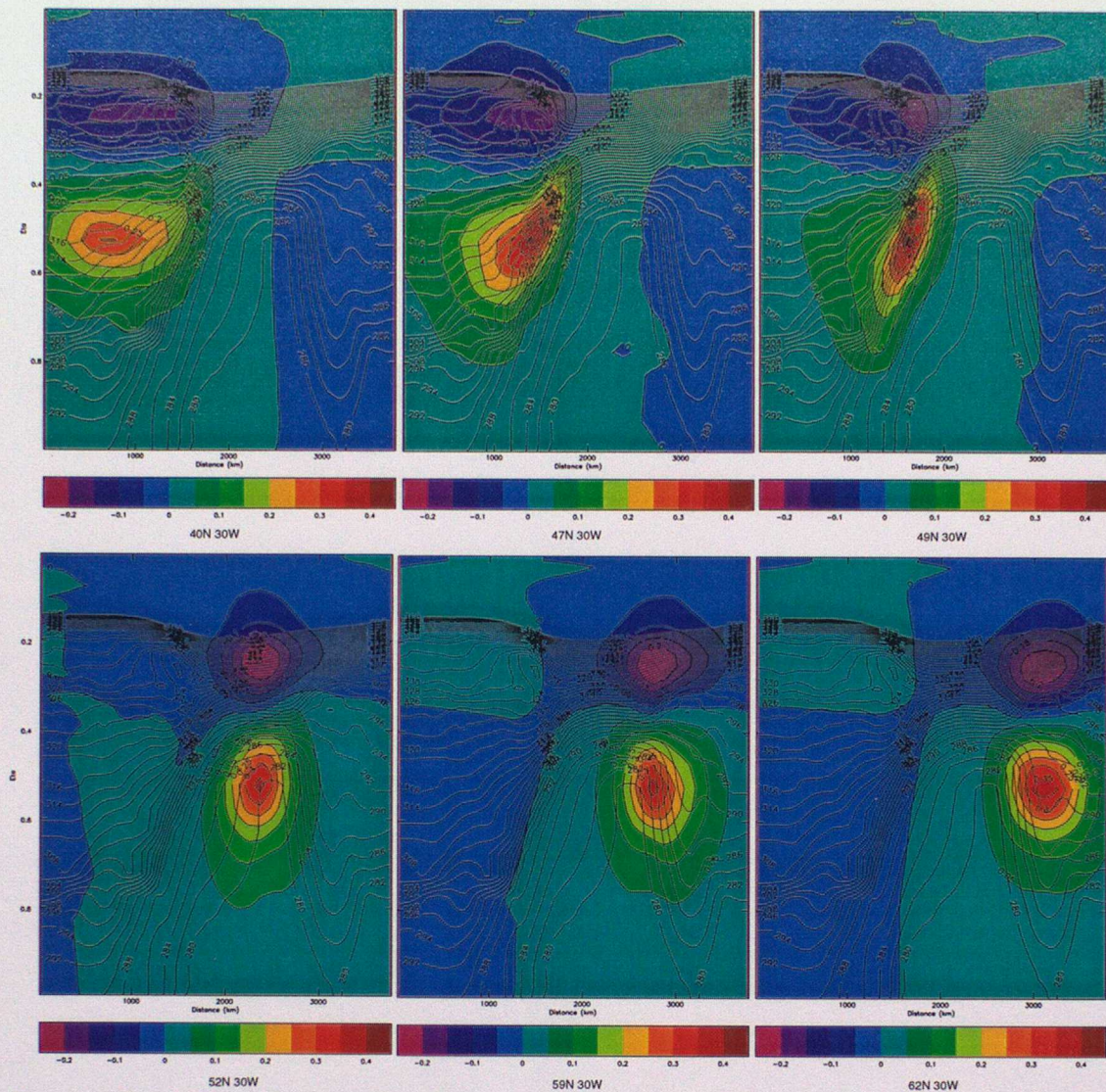


Figure 4 Behaviour of the GCT on VAR near a frontal zone (θ_1 analysis increments). Identical cross sections have been taken south to north along 30W in all cases (i.e. different cross sections to that taken earlier). The single observation is specified further north each time (top left to bottom right) so that the assimilation takes place initially in the warm sector (top left), through the strongly baroclinic region (top right), and out into the cold sector (bottom right).

2.3 Specifics of the EotD

Considering the EotD system, the θ_1 bredmode structure on model level 11 for this analysis time is shown in Figure 5, where there is a large negative area of bredmode activity located across the frontal region from west to east. A cross section through this region shows that the structure extends throughout the troposphere and exists largely on the warm side of the frontal zone. This is consistent with the aim of the EBS, in that it is designed to identify regions of rapid growth in the previous time steps, and one would expect that this would be a characteristic of developing or decaying frontal regions. Furthermore, the bredmode exhibits some degree of the flow dependence up the frontal zone that is exhibited by the GCT. This is presumably due to the fact that bredmode structures originate from forecasts generated from perturbed analyses, and therefore they contain all the flow dependence and balance constraints of the model from which they are derived.

If the profiles of the θ_1 bredmode structure shown in Figure 5 are compared with the relevant profiles of analysis increments in Figure 2 and Figure 3, it is apparent that there is a similarity between the distribution of information within the bredmode profiles and the distribution of the increments within the VAR analysis. Also, the magnitude of the bredmode structure is relatively intense in the central and upper part of the distribution, and this corresponds with the larger area occupied by the higher magnitude analysis increments.

These correlations are a good indication that the EBS is being used as intended to modify the VAR analysis, and the observed structure of the bredmode in this example shows good meteorological behaviour.

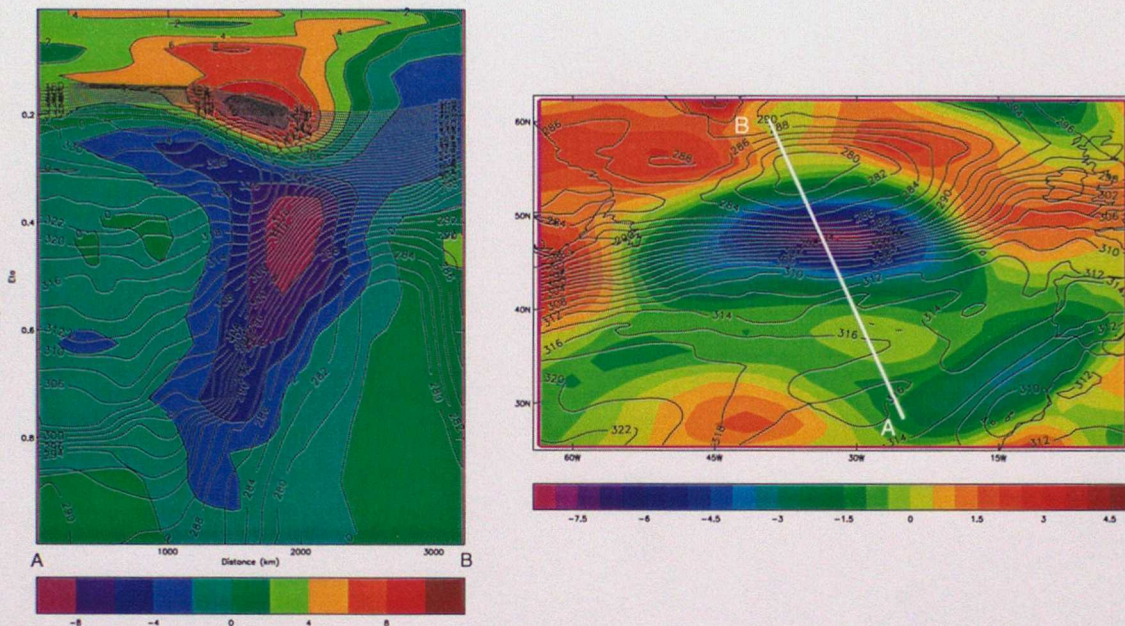


Figure 5 Cross section (left) through the θ_1 bredmode structure on model level 11 (right). The black contours show the UM θ_1 analysis (plan view on model level 11).

The single observation test discussed above and shown in Figure 2 and Figure 3 was repeated using a larger θ increment of 4K (instead of 1K) to investigate whether the results were dependent on the magnitude of the assimilated observation. It was found that the intensity of the analysis increments increased in proportion to the magnitude of the pseudo observation in all three cases, although some deficit was evident (i.e. with $\theta=1K$, maximum increment ~ 0.4 , with $\theta=4K$, maximum increment ~ 1.2).

The distributional behaviour of all three assimilation schemes did not change relative to each other in both the horizontal and vertical when the magnitude of the pseudo observation was changed in this way. It was also found that the boosting of analysis increment values for the EotD scheme relative to the VAR and GCT schemes on model level 11 remained. This is a good indication that the influence of the bredmode on the distribution of the observation increment is independent of the magnitude of the increment.

2.4 Propagation of GCT and EBS Effects in Data Analysis

The pseudo Single Observation tests shown in the preceding sections consider the output of VAR as the VAR increment field. This field is therefore represented on the Arakawa-C Charney-Phillips grid with 216×163 resolution and 30 levels in the vertical. In the operational model, this field is used as input by the Incremental Analysis Update (IAU) from which it is incorporated with the relevant background field in order to initialise the UM. This step from VAR increment field to IAU increment field therefore involves a change of grid from the VAR (Arakawa-C Charney-Phillips) grid to the UM (Arakawa-B Lorenz) grid.

In order to investigate whether the results of the VAR analyses were being preserved through changes in grid resolution, the GCT increment field shown in **Figure 3** (middle) was examined on both model grids (Figure 6). The results show that there are some minor modifications to the increment field as a result of changes in the model resolution. For example, the small region of maximum increment in the VAR field is represented as a single region of the same magnitude in the UM field (this is presumably a direct result of the change in vertical staggering in the two grids). There also appears to be minor alterations to the distribution in other regions, and an overall lower altitude for the increment field in the UM compared to that in VAR.

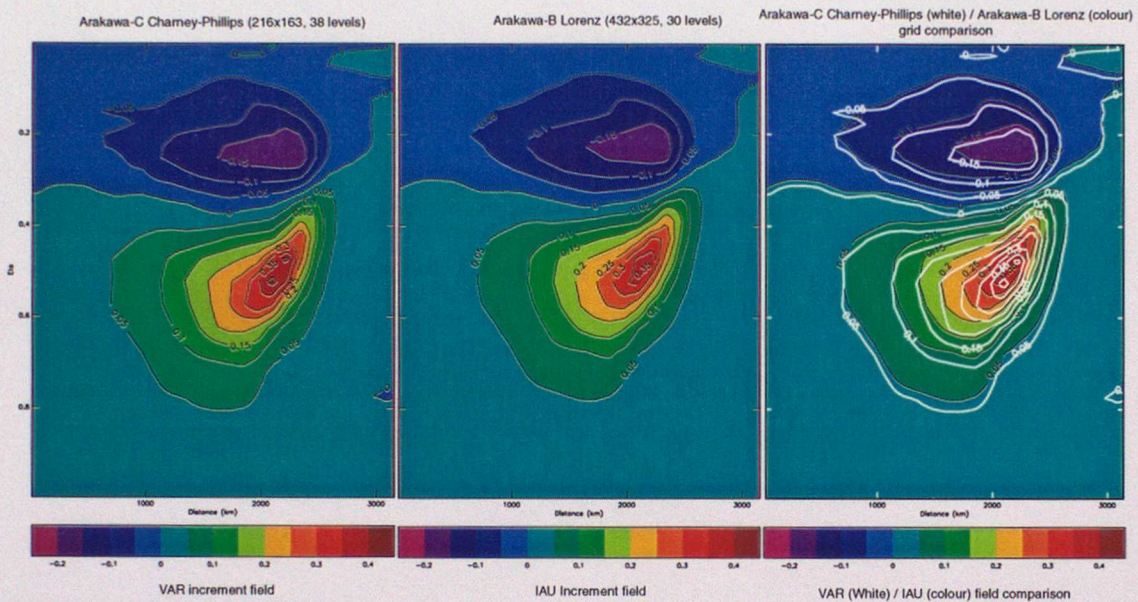


Figure 6 The θ_1 analysis increment field for a pseudo single observation, displayed on both the VAR (left) and UM (middle) model grids. The figure to the right shows the UM increment field compared directly with the VAR increment field in white contours.

However, although this study shows that there is a detectable change brought about when converting from the VAR to UM grids, none of these differences would be expected to cause any significant decrease in performance of any of the schemes.

This test shows that modifications brought about by the GCT and EBS do pass through the IAU stage of the analysis procedure. In order to test if there is any impact on Unified Model forecasts brought about by the GCT and EotD, the PF analysis fields created by the single observation test shown in Figure 2 and Figure 3 were used to run T+24, T+48 and T+72 hour forecasts (as shown schematically on the right of **Figure 1**). In this study, temperature on the 500hPa pressure level was used to detect any deviations between the forecasts generated when either the EotD or GCT were either active or inactive.

Figure 7 shows 500hPa temperature difference fields generated from the assimilation with GCT active (VAR+GCT) and the assimilation with GCT inactive (VAR). It was found that minor differences relative to the VAR-assimilated run were observed for the first 24 hours. By 48 hours differences of the order of 0.3K were observed for the GCT run, located primarily along the frontal zone on which the single observation was placed. At T+72 hours, the differences had grown to ~1K again primarily along the frontal zone.

The same experiment was repeated for the case in which EotD had been used to modify the pseudo single observation. In this case, the differences of the GCT run relative to VAR were slightly greater in magnitude and extent than the differences of the EBS run relative to VAR, although both showed the same general pattern, and both deviated from the VAR runs in similar locations. It should be noted however, that the size of the modification brought

about in the EotD case will be highly dependent on the size of the bredmode in the particular location of the obsevation, and so the impact of the EBS on the analysis will vary from case to case.

This experiment shows that even minor changes to the data analysis brought about by the GCT and EotD systems are propagated through the forecast system. The next part of this report investigates the impact of these schemes on operational forecasts.

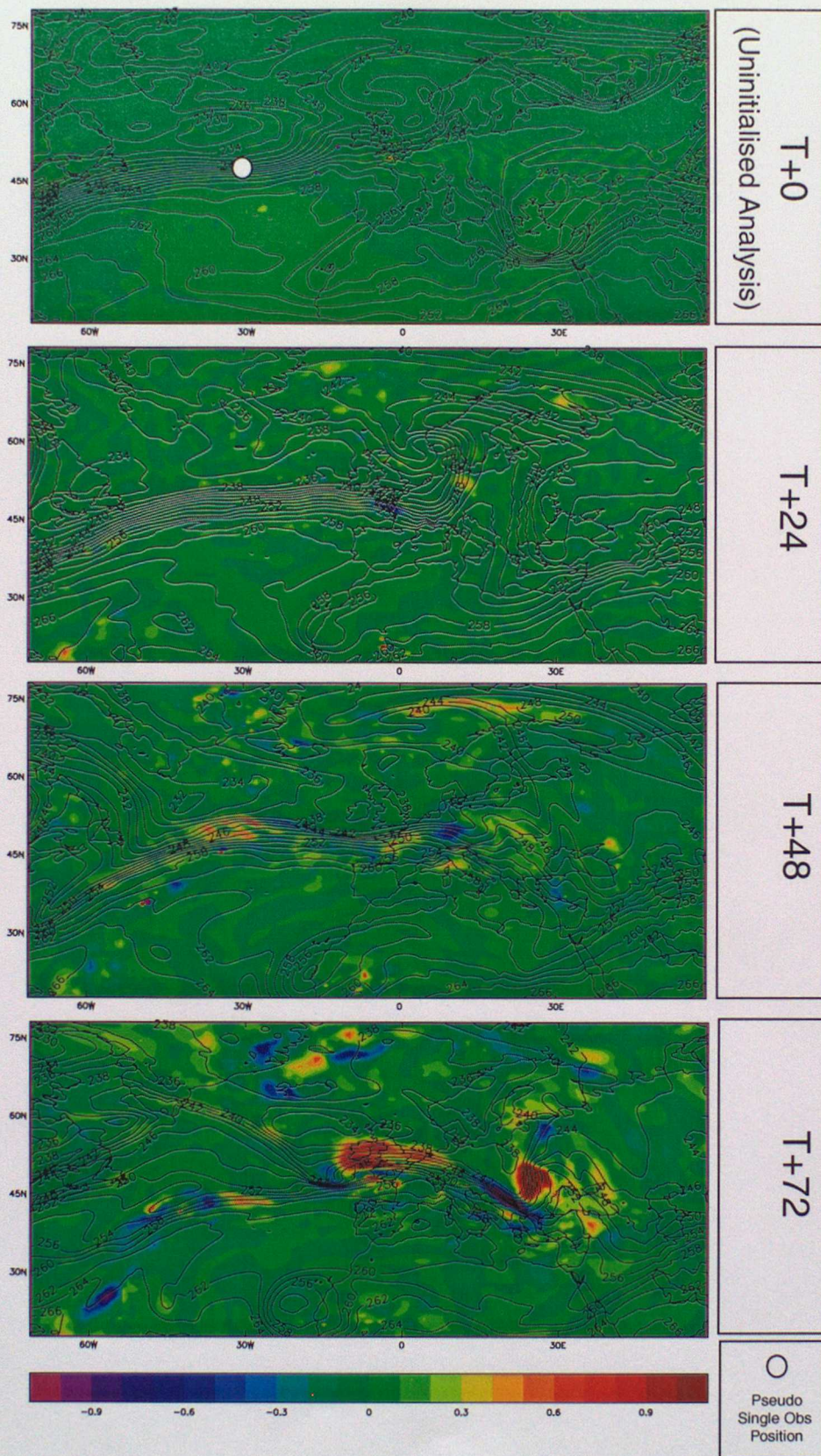


Figure 7 (VAR+GCT) – (VAR) 500hPa temperature forecast difference fields (colour) generated from Pseudo Single Observation test with GCT active (Figure 2). Contours show temperature at 500hPa from the control trial analysis.

3. Impact Assessment of the GCT & EotD on Individual cyclogenesis UM Forecasts

This section documents in detail an assessment of how the GCT and EotD assimilation schemes affected the development of individual cyclogenesis events within two regions of the globe on one particular day. Each case study deals with the development and evolution of more than one cyclone. The case studies for this investigation were taken from the GCT and EotD trials discussed in section 1.1.

The verification suite is designed to give an indication of how well each trial is performing relative to its own control trial, and is displayed as RMS errors within selected regions. Initially this information was used to choose relevant cases in which to study the effects of the GCT and EBS systems on the VAR analyses and UM forecasts. However, it was found that the sole use of this information could be misleading, presumably as the RMS scores are globally averaged.

Thus although this information was used as a guide, case studies in the first instance, were chosen purely on the basis of when and where cyclogenesis events were occurring. In later cases, the criteria were tightened to select only more mobile cyclones in the Northern Hemisphere. Finally, only mobile cyclones in the North Atlantic were analysed. This provided a good cross section of cyclone behaviour characteristics in which to test the different assimilation schemes on trial.

3.1 *Impact of the GCT and EotD on Operational VAR analyses, and their Effect on UM Forecasts*

It has been shown in the previous discussions that both the GCT and EBS have positive and relatively significant impacts on the way that observations are assimilated and that the modifications to the analysis brought about by the two schemes have a detectable effect on the model forecasts. Further, their effects on the pseudo observational information appear to be meteorologically sound. In order to test how each system behaves in an operational environment, a case was chosen at random from the trials in which a comparison of analysis increments could be made.

Figure 8 shows the global differences of the θ_1 analysis increment fields for the GCT and EotD schemes with respect to their respective control trials at 12z 21/12/99. Both schemes are capable of producing analysis differences of the same order of magnitude, and both systems seem to primarily produce modifications to the storm track regions of the northern and southern hemispheres (although the EotD system clearly results in more widespread changes).

Although both systems show concentrations of modifications within and around the storm track regions there is no strong correspondence between the modifications made by one scheme and the modifications made by the other. For example, there is no major difference between the GCT and control run in North America to the west and east of the Hudson Bay, whereas there are two large differences between the EBS and control run in these locations, with the one to the east extending into the North Atlantic as far as Iceland. The storm track region in the Southern Hemisphere is particularly affected by the EotD system, with an almost continuous sequence of modifications observable.

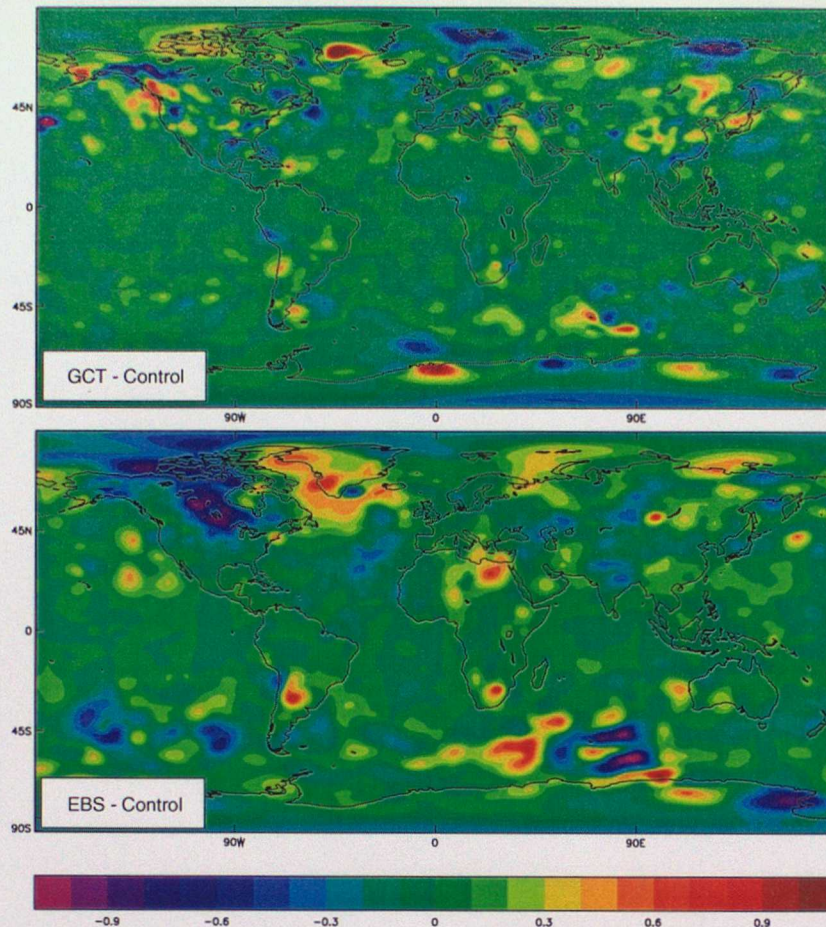


Figure 8 θ_1 (model level 4) analysis differences for GCT and EotD (EBS) systems relative to their control runs, 12z 21/12/99.

These observations do not show superiority of one scheme over the other as each scheme is designed and has been shown by the single observation tests to be playing a different role in the modification of the VAR increment field: in areas of modification, the GCT is incorporating better flow dependence into the assimilation of the observation, whereas the EBS will be varying the extent of the observational influence in response to the degree of variability of the background field in the recent past.

The impact of these modifications made by the GCT and EBS systems can be assessed by a comparison of forecasts starting from this analysis time. As an experiment, it was decided to study the performance of the 3 day forecast trial output in the location of significant analysis changes (neglecting areas such as Greenland where there may be anticipated problems due to the landmass) for each scheme. For the GCT scheme, an impact of high magnitude was located near 180 degrees west in the north Pacific Ocean, whereas the EotD scheme showed maximum impact in the Southern Indian Ocean (the GCT also shows significant modification in the same area of the Indian Ocean, and this was dealt with in a separate case study as a useful comparison of the two schemes).

3.2 GCT case study based on Maximum Analysis Modification, 12z 21/12/99

3.2.1 Analysis Changes

Figure 9 (top and bottom) show the θ_1 analysis increment differences in the region identified in section 3.1, where the largest effects of the GCT on the analysis have been observed at this time. Included on the difference plots are the mean sea level pressure contours (top) and the 850hPa θ_w contours (bottom) from the GCT control trial. Within this region of the Pacific Ocean, there are three extra-tropical cyclones labelled A, B and C where cyclone B is the origin of the largest GCT effect. To the east of the cyclones a large area of high pressure exists which builds over the coming three days and influences the track of the cyclones as indicated by the arrows in Figure 9.

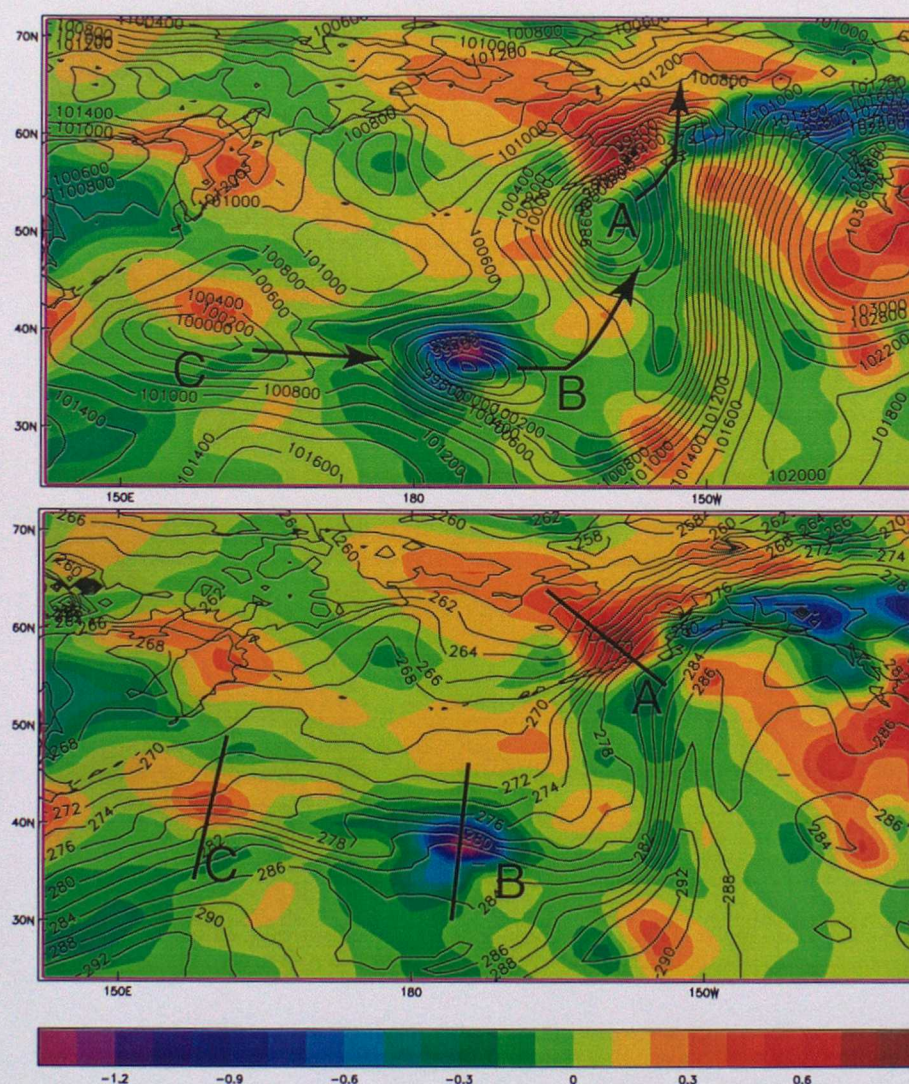


Figure 9 θ_1 analysis increment differences (GCT-Control) and mean sea level pressure (top) and 850hPa θ_w (bottom) contours, 12z 21/12/99. There are three cyclones present in this area (A,B,C) with their trajectories shown by the arrows in the top panel. The largest analysis difference produced by the GCT is associated with cyclone B and was identified as the largest effect of the GCT across the globe at this time in Section 3.1. Cross sections through the regions of large GCT effect have been taken along the lines indicated in the lower panel and are shown in Figure 10. Arrows indicate the future track of the cyclones over the following 3 days.

The origin of these analysis differences are illustrated in **Figure 10**, which shows cross sections across the lines shown in **Figure 9** (bottom). The impact of the GCT in each case may be observed by comparing the top and lower rows.

For cyclone A the θ_1 analysis increments at mid levels and to the north are observed to change their orientation to better reflect the proximity and slope of the frontal zone. The increment at low levels and to the south is observed to be reduced in vertical extent but increased slightly in horizontal extent. The GCT in this case is therefore observed to be redistributing the increment information along the frontal planes.

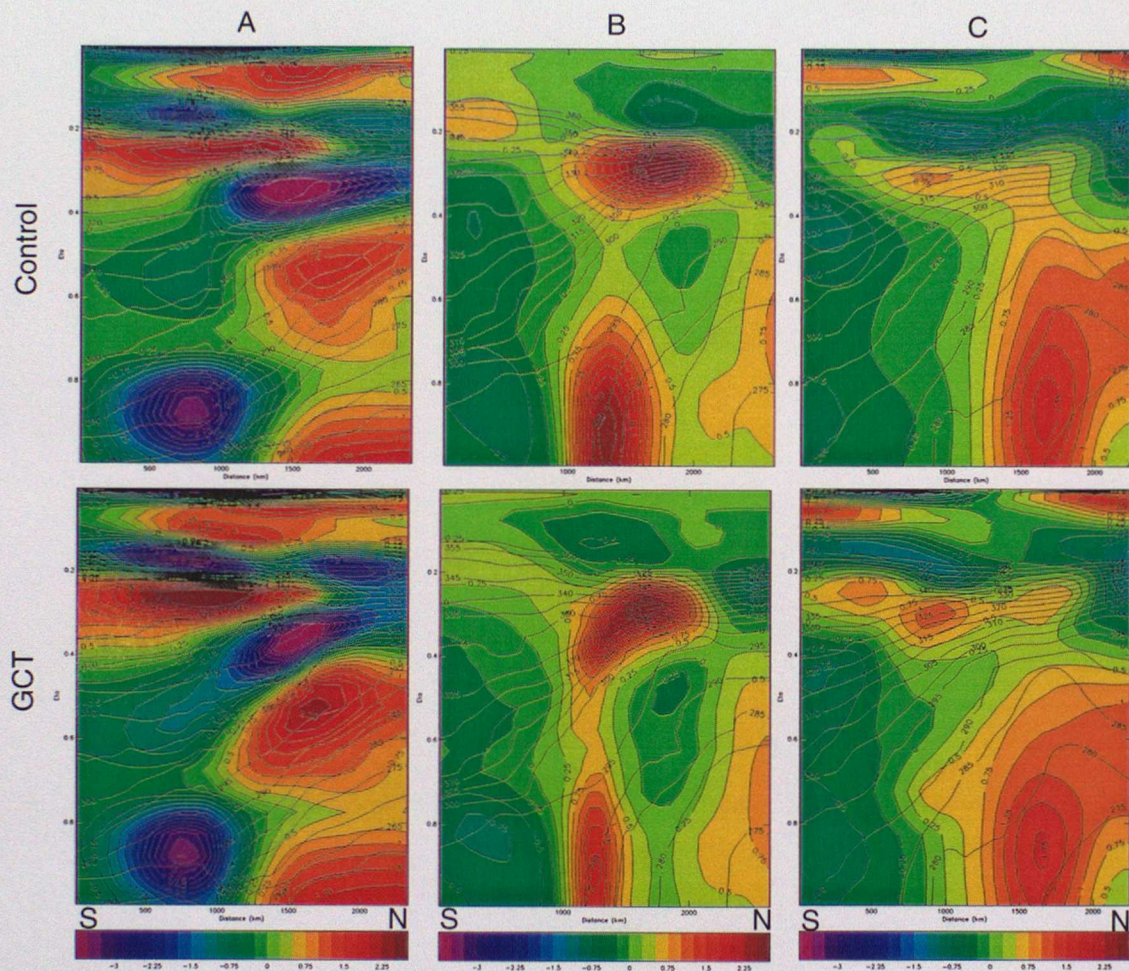


Figure 10 θ_1 analysis increments for the Control (top) and GCT (bottom) trials on model level 4 for cyclones A,B and C shown in **Figure 9**. Contours show the operational θ_1 distribution on model level 4. Overall, the GCT has the effect of boosting many analysis increments and incorporating a flow dependence in regions of baroclinicity.

Cross sections through the analysis increments of cyclone B show that there are two areas of modification brought about by the GCT in this location. The first is a low level modification to the frontal zone where it extends towards the surface. The GCT has the effect of not only reducing the magnitude of the increment, but also horizontally and (to a lesser degree) vertically reducing its extent. The reduction in horizontal extent of the GCT increment effectively means that information from the one side of the front is distributed to a lesser degree across the front. This is a desirable feature for the GCT scheme to have, as the effect of this on the analysis would be to lessen any tendency which VAR increments may have to attenuate the front, so helping to maintain the integrity of any frontal system near an observation in the final analysis.

The second area of modification in this location is to an analysis increment at upper levels (compare middle top and middle bottom, **Figure 10**). The VAR system produces an oblate

shaped analysis increment lying horizontally and bounded by the tropopause. The GCT has the effect that the increment is more flow dependent, and the increment respects the frontal characteristics of this region.

Cyclone C shows a more subtle effect of the GCT as the magnitude of these changes are ~ 0.3 times the magnitude of those observed for cyclone B. The GCT shows a slightly reduced vertical extent at low levels to the north, but an increment of increased magnitude at upper levels to the south. The orientation of the increment at upper levels is also adjusted by the GCT so that its orientation lies along the slope of the frontal zone.

All these changes show a success of the GCT scheme. Together, they illustrate greater flow dependence, a correlation between modifications and baroclinicity, and a reduction in the smoothing out of baroclinic zones that VAR can sometimes produce in its increment field. In the next section the impact on the forecast by these modifications will be addressed.

3.2.2 Forecast Changes

Within 24 hours of the analysis time discussed in section 3.2.1, cyclones A, B and C have moved as indicated by the arrows in Figure 9, with cyclone A situated over Canada. The mslp fields for 12z 22/12/99 are shown in Figure 11 which compares the accuracy of the T+24 forecast relative to its verification analysis.

For Cyclones A and B there is no significant difference between the performance of the forecast in either the Control or GCT Trial runs. Cyclone A is developed similarly in both position and depth in both runs, with no significant difference in central surface pressure. Both runs also develop only one cyclone associated in the cyclone B area, whereas the verification analyses show that two cyclones have evolved in this time period. Cyclone C shows some evidence of differing development, however. The mslp difference between the forecast and analysis for the control run is 4.3mb, whereas that for the GCT run is 2.5mb; reducing the mslp forecast error by ~40%.

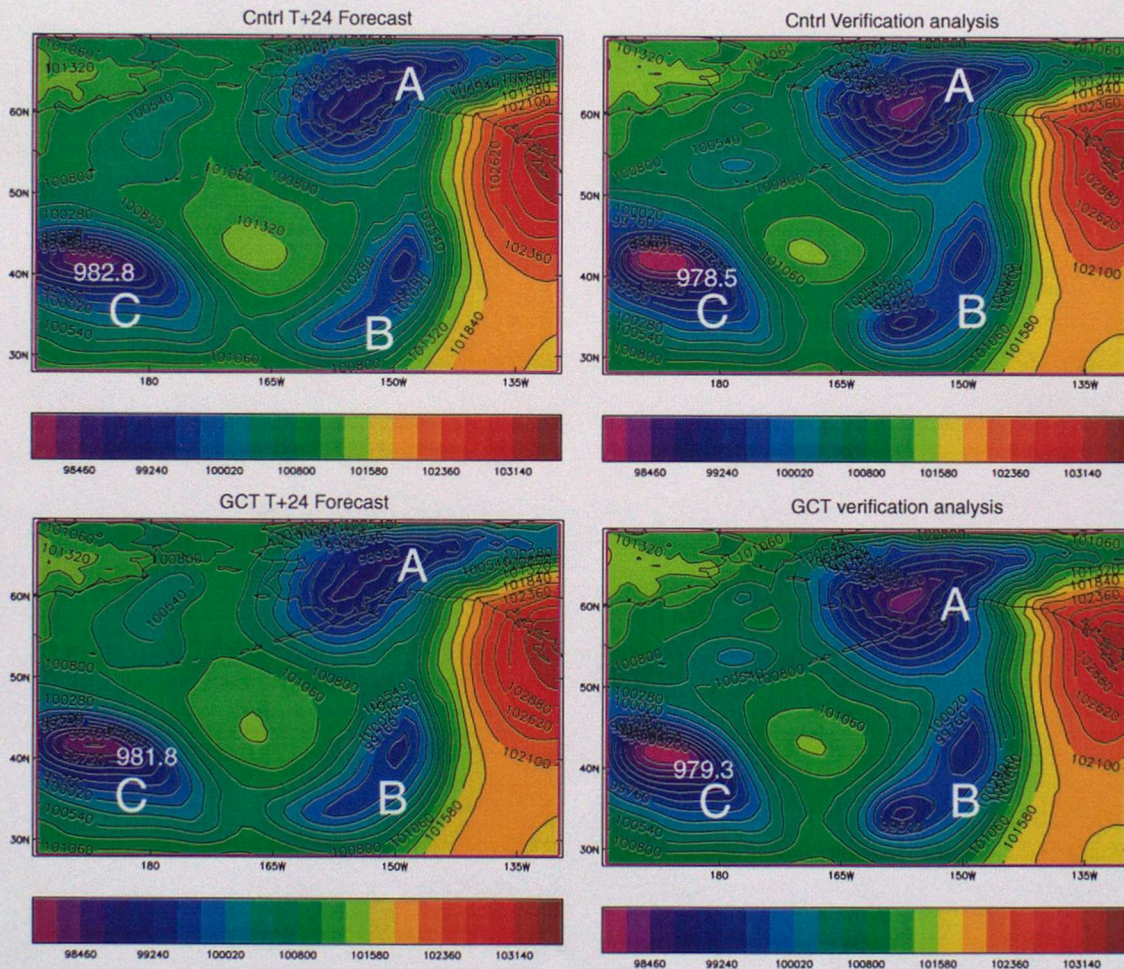


Figure 11 Mean Sea Level Pressure (Mslp) fields for 12z 22/12/99. The fields compare the accuracy of the T+24 forecast relative to its verification analysis for both Control and GCT Trials.

The T+48 forecast (mslp fields not shown) continues this trend. Cyclone A fills in this period and so is considered no further as does the northern cyclone in the Cyclone B area (Figure 11). The southern component of cyclone B has also begun to fill but is still an active low pressure system. The difference between the forecast central low pressures of cyclones B and C is observed to be very small. In the T+72 forecast fields (not shown), B has filled completely and is no longer active. Cyclone C has deepened further. The difference

between the central low pressures in the control run is 2.7mb, whereas that for the GCT run is 1.3mb, reducing the mslp error by about 50%. A marginal improvement in cyclone C's position could be argued in the T+72 GCT forecast relative to that for the control forecast.

As the GCT is so intimately connected to frontal zone development, it is useful to examine whether or not there is any signal of GCT activity in the precipitation rate. The model precipitation rate fields for the control trial are shown in Figure 12, and those for the GCT trial are shown in Figure 13. A relative comparison of the two figures allows an assessment of the performance of the GCT in terms of its effect on precipitation rates to be made. The figures show that both the precipitation rates and distributions are forecast well for cyclones B and C in the control T+48 forecast (c.f. (a) and (c) on Figure 12). In the case of cyclone B, the control run performs better relative to its own verification analysis than the GCT, as the GCT has had the effect of suppressing the precipitation in the GCT forecast (c.f. (a) and (c) in Figure 13). Cyclone C is forecast reasonably well in both the control and GCT runs, although the GCT run correctly represents the frontal rain band as a tighter structure (the control run rain band appears more diffuse).

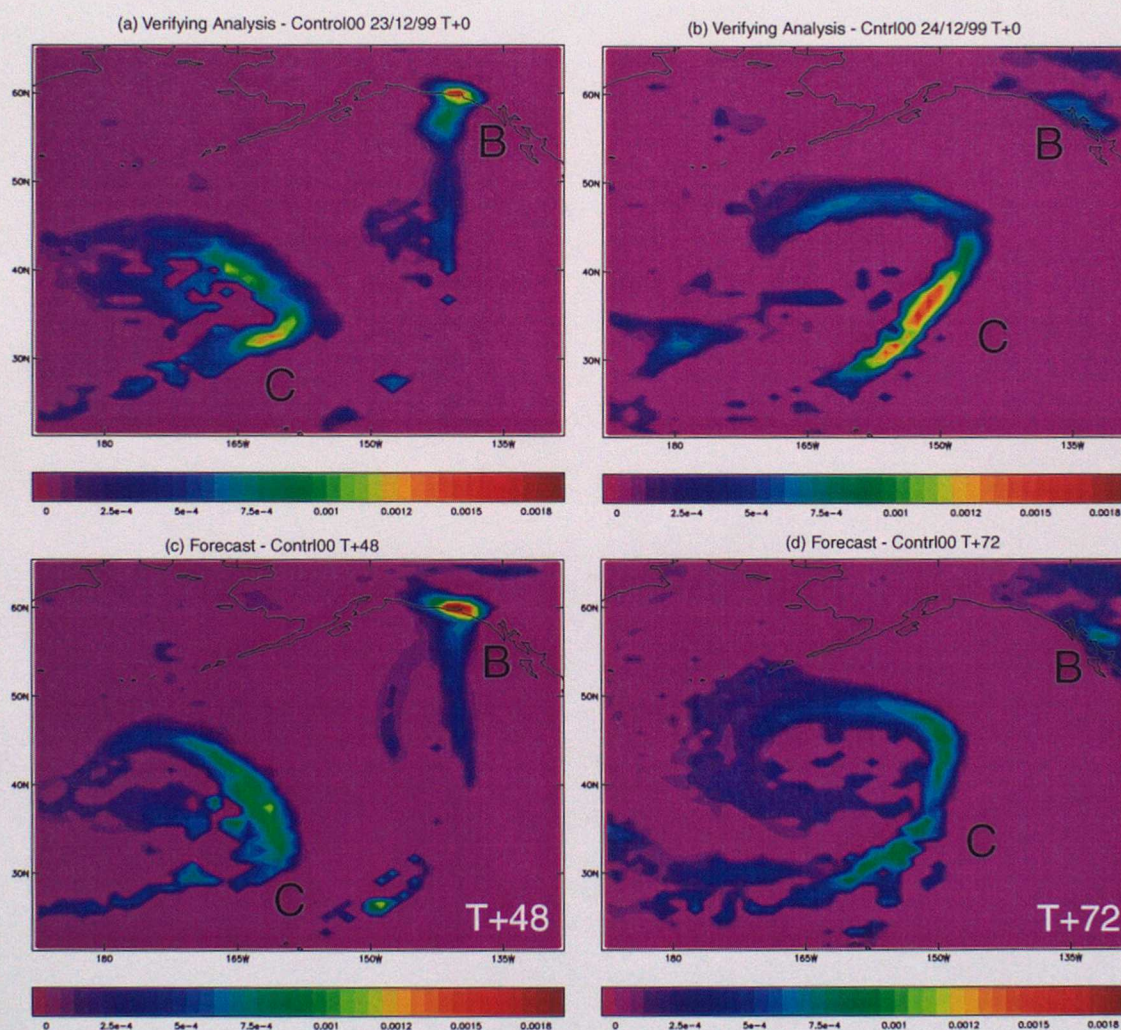


Figure 12 Control Trial Model Precipitation rate ($\text{Kg/m}^2/\text{s}$) for 12z 23/12/99-24/12/99. The top row shows the verifying analyses. The bottom row shows the forecasts T+48 and T+72 from 12z 21/12/99. By these times, both cyclone B has begun to fill and show increasingly less precipitation, whereas cyclone C is undergoing development. In the T+48 forecast the precipitation rate within system C to is under-estimated and is represented by a wider band than in the verifying analysis. The T+72 forecast shows a significant under-estimation of the precipitation rate in the trailing cold front C.

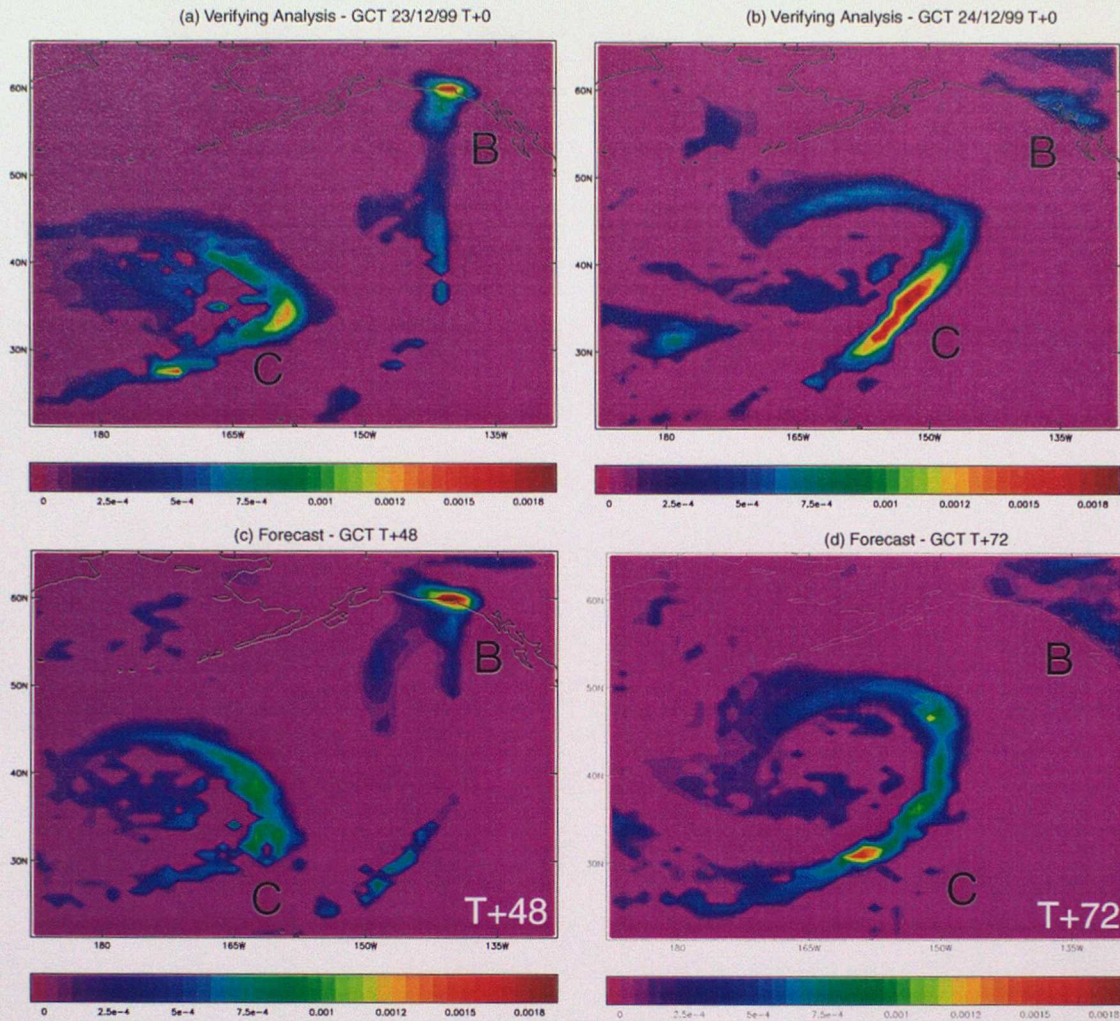


Figure 13 GCT Trial Model Precipitation rate ($\text{Kg/m}^2/\text{s}$) for 12z 23/12/99-24/12/99. The top row shows the verifying analyses. The bottom row shows the forecasts T+48 and T+72 from 12z 21/12/99. By these times, cyclone B has begun to fill and show increasingly less precipitation, whereas cyclone C is undergoing development. In the T+48 forecast, although the precipitation rate of cyclone C is under-estimated, the frontal zone is noticeably tighter and closer to that of the verifying analysis. Relative to the T+72 control forecast the precipitation rate of cyclone C is much better represented with increased values down the main frontal zone. The vortex of the system also appears to be better represented in the T+72 GCT forecast than in the T+72 control forecast.

In the T+72 forecast the control run significantly under-estimates the precipitation rate through the main frontal cloud band of cyclone C trailing in a NE/SW direction (c.f. (b) and (d) on Figure 12). The showery precipitation within the vortex region of cyclone C appears over-estimated relative to its verification analysis.

The GCT performs better than the control run for the T+72 forecast. The under-estimation of the precipitation rate observed in the control run has been rectified somewhat by the GCT as can be observed by the increased precipitation in the frontal rain band (c.f. (b) and (d) in Figure 13). Relative to its own verification analysis, the showery precipitation in the vortex region of cyclone C is better represented. Although the distribution of this precipitation is different in both analyses (Figure 12(b) and Figure 13(b)), one would generally expect significant showers in this region. This suggests that Figure 13(b) is likely to be more representative of the real atmosphere than Figure 12(b) and that overall, the GCT has significantly improved the precipitation rate forecast.

3.2.3 Overall Assessment of the GCT in this Case Study

The GCT has been shown in this case study to have a positive effect on the VAR analysis increments for the 3 cyclones in the vicinity of the maximum global effect on the analysis at 12z, 21/12/99. In all three cases associated with three cyclones A, B and C, the GCT was observed to introduce an observable flow dependence to the VAR increment structures. In some cases an intensification of the increment associated with a baroclinic zone was observed and is likely a result of the redistribution of the VAR increments according to the Geostrophic Co-ordinate Transformation. This redistribution of observational information in this way is consistent with that observed in the SOTs discussed in section 2.

The modifications brought about by the GCT to the analysis produce no significant alterations to the forecasts of cyclones A and B, but are observed to improve the mslp forecast of cyclone C. This is surprising in that cyclone C had the smallest GCT activity in the 3 cyclones studied with modifications ~0.3 times the magnitude of those observed for cyclone B.

Further, the GCT was observed to improve the forecast precipitation rate fields for cyclone C. The effect was a tightening of the precipitation along the frontal zone in the T+48 forecast and a strengthening of the precipitation rate in the T+72 forecast. This provided a favourable comparison with the verification analyses. The GCT was observed to have a negative effect on the precipitation rate fields for cyclone B, causing a degrading and weakening of the precipitation in the T+48 forecast relative to the control verifying analysis.

This case study shows that the role of the GCT is a subtle affair in that the magnitude of the modification of the VAR increment fields, and the subsequent modification of the UM analyses does not necessarily translate to the magnitude of modification on the UM forecasts. There is clearly an underlying sensitivity in the model dynamics to the activity of the GCT that is yet to be identified.

3.3 EotD Case Study based on Maximum Analysis Modification, 12z 21/12/99

3.3.1 Analysis Changes - Verification of the EotD Operation

The maximum impact of the EotD scheme on the analysis was observed to be in the southern Indian Ocean. In this location, there exists a series of relatively large modifications to the analysis that extend west to east from the southern tip of Africa towards southern Australia (Figure 8). The negative modification to the east is in the vicinity of a cyclone heading SE whilst the positive modification to the west is in the vicinity of a developing cyclone heading due east.

This case study considers the analysis and forecast evolution of these two cyclones. At the analysis time (12z, 21/12/99) the first of the cyclones lies to the north of Antarctica at approximately 40E, and is at a relatively early stage in a cyclone's evolution. This is the cyclone that is associated with the large positive analysis differences in Figure 8. The second cyclone, at a much later stage in a typical cyclone's development, is situated further to the east at approximately 90E, and is associated with the large negative region in Figure 8.

The EotD modifications that led to the analysis differences are shown in Figure 14.

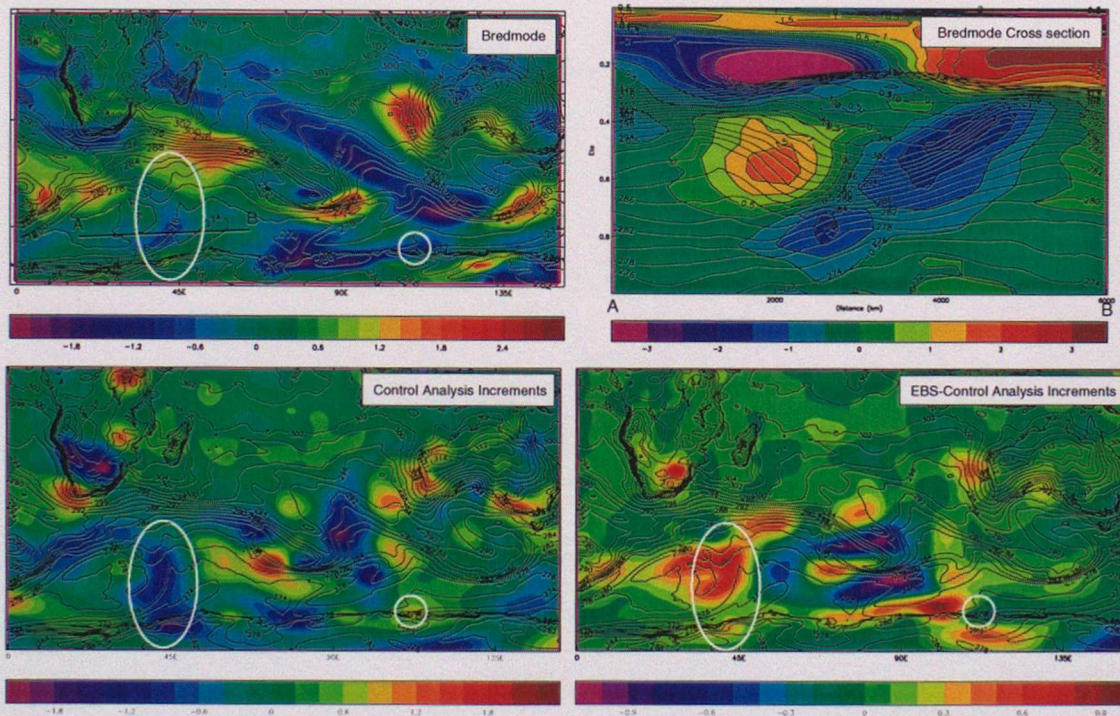


Figure 14 The effect of bredmode activity on analysis increments, 12z 21/12/99. The top left panel shows the θ_1 bredmode structure on model level 4, whilst the top right panel shows the cross section through AB of the bredmode. Bottom left shows analysis increments for the control trial and the bottom right panel shows the difference between the EotD and VAR assimilation systems on the analysis increments. Contours are the θ_1 field from the operational model. White circles and ovals are referred to in the text.

The θ_1 bredmode structure on model level 4 (top left) shows that most bredmode activity is along regions of strong baroclinicity and this is a good indication that the EBS is working as anticipated (see discussion on SOT's, Section 2). The cross section AB (top right) cuts

through the bredmode structure which is in close proximity to the developing low pressure system near 40E. The behaviour observed in both the single observation test and the earlier EotD case is borne out again in this cross section: the bredmode activity is collocated with the frontal zone, and shows very good flow dependence, thereby conserving any frontal system that may be represented in the model (the discussion which follows will show that this is influential in the positive impact on the forecast). The two lower panels on the figure show the analysis increment field (θ_1 , model level 4) for the control run on the left, and the regions of analysis increment differences between the EotD run and the control run on the right.

The presence of control analysis increments in any area indicate that observations in that area differ from those values forecast in the background field, and so modification to the background field is required in order to produce the analysis. Absence of control analysis increments can mean that (a) observations are precisely as forecast (in the background field) and so modification of the background field is not required or (b) there are no observations in this location for VAR to establish a deviation of the background field from the observation.

The following discussion examines the operation of the EotD scheme by comparing the bredmode structures and analysis increments of Figure 14 with the location of surface observations taken during the analysis time.

Surface observations taken by ship, buoys or land stations within three hours of the analysis time were considered (extracted from the MetDB) as an indication to whether or not statement (a) or (b) above was true. Consider, for example, the difference indicated along the northern coast of Antarctica, centred on 100E. Observations (not shown) along this coast are very sparse, except for a high density within the circled area on the figure (presumably the position of a seaport). The control analysis increments within this circle confirm the position of this port and indicate that statement (a) is the case in which there are observations which deviate from the background field and therefore produce an analysis increment centred on the port. The EBS-Control difference field within this circle is zero, indicating that the EBS has had no effect on the observations at their true location within the standard VAR distribution. However, there are large and significant areas of differences visible in this field to the west of the circle (extending out along the coast to approximately 70E), indicate a high impact of the EBS along this area. This pattern of differences is identical to that of a bredmode structure (top left of figure), and confirms that given observations within a region occupied by suitable bredmode structure, the EBS acts as designed so as to extend the observational information within that area.

Consider the developing cyclone discussed earlier and situated at approximately 40E. The location of this is in close proximity to the bounded region within the white oval on Figure 14. The control analysis increments in this region extend from the north coast of Antarctica northwards, the pattern of which is a result of a number of observations made (presumably) in a seaport on the coast, and a small number of buoys and ships to the north (not shown). The bredmode activity in this location is relatively small, but is concentrated around a sharp frontal zone running roughly parallel with the Antarctic coastline (Figure 14, top left), and inclined slightly to the north at its east end.

The effect of the bredmode activity in this case is to horizontally restrict the observational information made by the ships and buoys to the north far more than would be used in VAR alone, and to spread the information more intelligently vertically up the frontal zone as indicated by the cross section in Figure 14. The result would be less weakening of the frontal region (as may occur with VAR via the smoothing of the analysis increment) and a sharper baroclinic zone in the analysis. The result of this will be shown in the next section to be an improved forecast in central surface pressure and location of the cyclone, and represents confirmation that the EotD process is working as intended.

The large differences due east of the oval and midway between the oval and the circle on the figure are associated with the modification in the analysis of the second cyclone, situated at 90E (refer to Figure 15). A similar analysis to that carried out above in this location has shown that these differences are in a highly data sparse area, and that they appear to be due to the modification of observations made by two isolated buoys; one to the far north of the front and one to the far south. The modifications appear to be distributed in accordance with the principles discussed elsewhere in this report, and in accordance with successful modifications in other cases. The following section will show that only marginal improvement in position was observed for this cyclone, with no significant increase in forecast accuracy of the central surface pressure.

3.3.2 Forecast Changes

A comparison of the 3 day forecast for each cyclone with the control analysis at the verification time is shown in Figure 15. This is a relatively complex synoptic situation in which three cyclones exist at the verification time in the analysis (left of figure). The two cyclones identified earlier are indicated by the crosshairs (solid and dotted) in Figure 15. A third smaller cyclone, to the north east of the system to the west has also developed.

The EBS is observed to have a positive impact on the system to the west at the verification time, improving both its position (further to the SE, towards the solid crosshairs), and its central pressure; a 5mb error relative to the control analysis is reduced to a 2 mb error. The system to the east shows only marginal improvement in position (slightly more towards the dotted crosshairs) with no significant improvement in accuracy in the forecast central surface pressure.

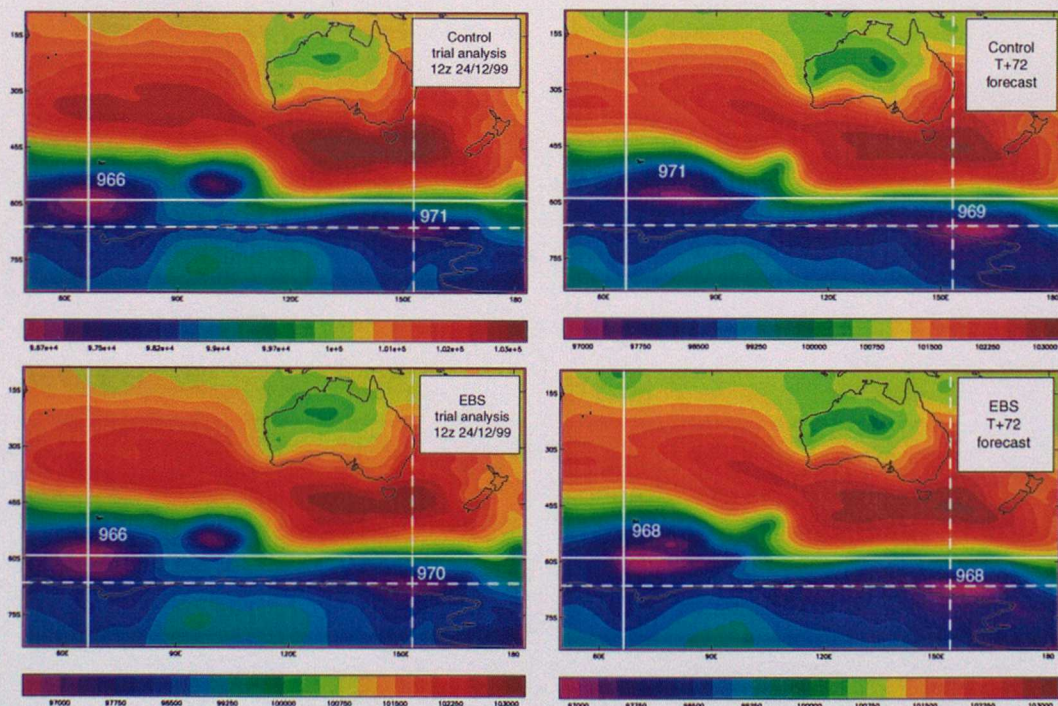


Figure 15 EBS/VAR 3 day forecast comparison, mslp. All fields valid at the verification time of 12z, 24/12/99. The solid cross hairs show the position of the western low pressure system in the control analyses, whilst the labels refer to the central low pressure. The dotted cross hairs show the position of the eastern low pressure system in the control analysis. The EBS system has resulted in an improved position and improved central surface pressure relative to the control trial. There is no significant change in the forecast position of the forward low pressure system.

The precipitation rate for the EBS forecasts (not shown) were verified against those produced from the control run. For the cyclone to the west, it is difficult to compare the T+72 forecasts with their verifying analyses due to the absence of the third cyclone in the model fields. The presence of this cyclone distorts the baroclinic zones around the main cyclone to the west so that precipitation fields are too different to compare. Nevertheless the shift in position of the western cyclone (towards the crosshairs on the figure) is sufficient to better predict the position of the frontal rainband to the south of that cyclone.

The cyclone to the east (as indicated by the dotted crosshairs), shows neither a degradation nor an enhancement of the precipitation rates.

3.3.3 Overall Assessment of the EotD in this Case Study

The EotD system has been shown in this case study to be working according to its design criteria. By extracting surface observational information from the MetDB, it was possible to verify that bredmode structural information was being used to vary the observational information in the correct way.

For the western cyclone in the case study it was shown that this bredmode activity was used to maintain the structural integrity of the baroclinic zone in this region resulting in an improved forecast for this cyclone. The improvement of the forecast related to both an improvement in the position and a reduction of the pressure error from 5mb to 2mb. A minor improvement to the cyclone to the far east was observed in terms of its position.

No significant effect was observed on the precipitation fields relative to the control forecast. Neither trial (with or without the EBS) correctly predicted the development of the third cyclone identified in the verification analysis.

This case was a stringent test for the EotD system in that cyclones were developing in an extremely data sparse region. However, this is in accordance with a design aim of the EotD in that it should make better use of existing observations particularly to improve the assimilation in such regions. This relationship between forecast accuracy, bredmode activity and observational information will be investigated in detail in a further case study in section 4.

3.3.4 GCT Impact in the same region

Although the maximum GCT effect in terms of modification to the analysis was found to be in the north Pacific, there were large and significant changes in the Indian Ocean in a similar location to that considered above for the EotD case study. The developing cyclones in this area were thus considered again as a GCT case study. For comparison purposes, the results are shown in Figure 16.

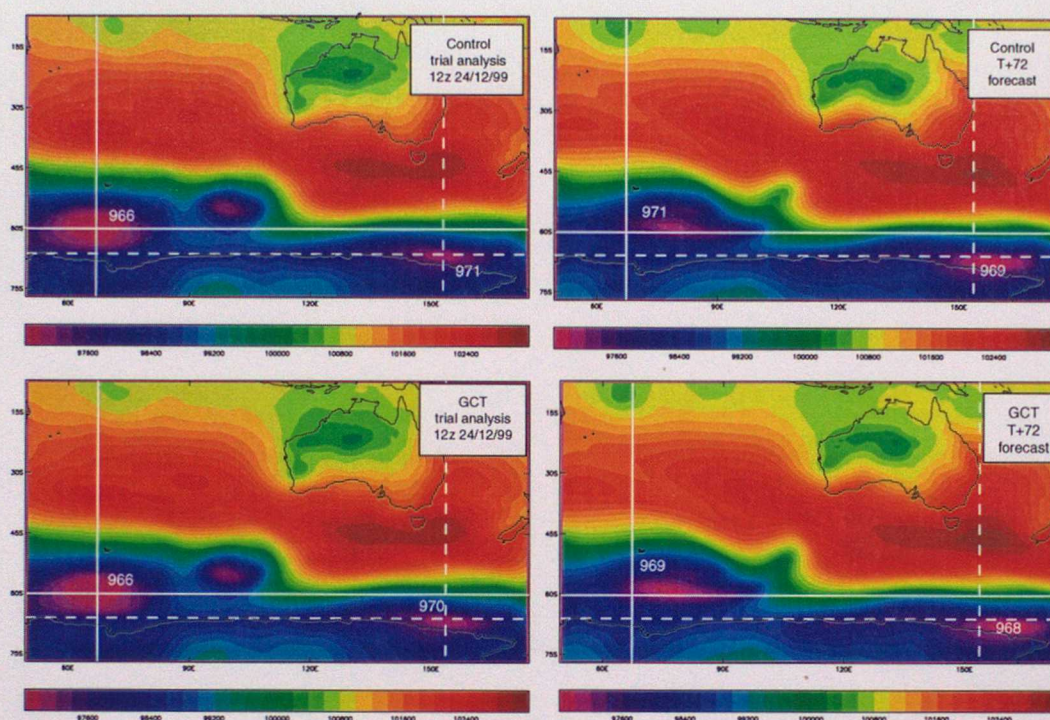


Figure 16 GCT/VAR 3 day forecast comparison, mslp. All fields valid at the verification time of 12z, 24/12/99. The solid cross hairs show the position of the western low pressure system in the control analyses, whilst the labels refer to the central low pressure. The dotted cross hairs show the position of the eastern low pressure system in the control analysis. The GCT system has resulted in a minor improvement in the central surface pressure of the western system relative to the control trial.

The results show that although significant changes have been made to the analysis in this location by the GCT (Figure 8), there is no significant impact on the positional errors in the forecast. The GCT is observed to reduce the mslp error of the western cyclone by 2mb to an error of 3mb.

No significant impact was observed on the precipitation fields in this case. However, this could be due in part to the non-development of the third cyclone as discussed in Section 3.3.2.

4. Bredmode Activity and UM Forecast Performance

The cyclone under study in this case developed on the trailing front of a cyclone that was situated to the north east of Iceland at the analysis time. The first sign of cyclogenesis was not observed in the analysis until a small surface low (997hPa) was observed south of Iceland at 12z 16th Dec. The cyclone then moved rapidly eastwards as it developed, crossing northern Scotland at 00z on the 17th (977hPa) and reaching Scandinavia at 12z on the 17th Dec with a central pressure of 967hPa. This case provided a stringent test for both the UM and the EotD scheme as the cyclone was of a rapidly deepening and rapidly moving nature and would therefore be expected to be highly dependent on the initial analysis.

Figure 17 shows the results of an investigation into the performance of the EotD system as a function of the intensity and extent of analysis increments produced by VAR. The left hand column of the figure represents the mslp analysis increments for 12z each day from the 14th to 16th December 1999. The pstar bredmodes from the EBS are superimposed on the analysis increments as contours (only the magnitude of bredmode maxima and minima are relevant). The middle column shows the mslp difference field between the control forecast (T+72, T+48, T+24) and the verification analysis at 12z 17th December. The contours represent the mslp verifying control analysis. The right hand column shows the mslp difference between the EBS forecast and analysis at 12z 17th December, with the contours representing the mslp verifying EBS analysis.

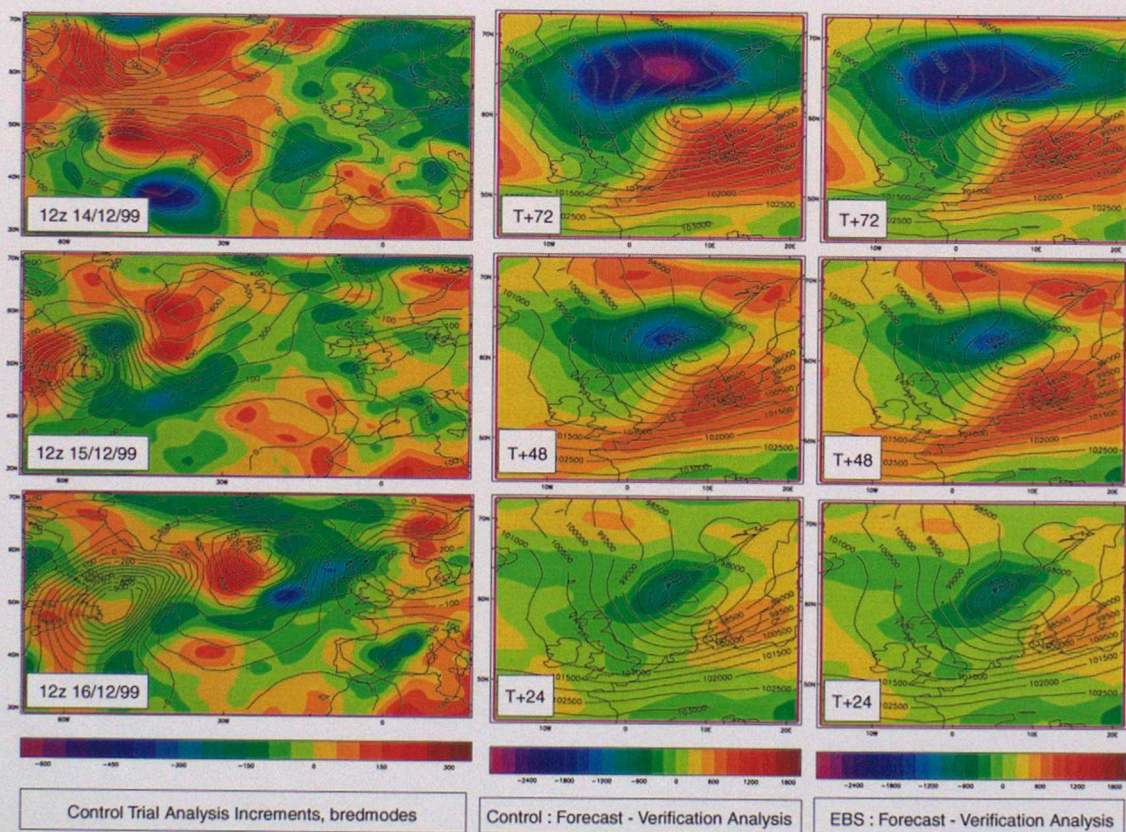


Figure 17 EotD performance as a function of bredmode activity and analysis increments. The left hand side shows the mslp analysis increments from the control trial in the north Atlantic region, with contours of pstar Bredmodes. The middle column shows the difference between the control mslp forecast and the control mslp verification time, with contours showing the control analysis mslp. The right column shows the difference between the EBS mslp forecast and the EBS mslp verification time, with contours showing the EBS analysis mslp.

On the 14th Dec, there is a bredmode structure situated on the south coast of Greenland. By extrapolating back the position and speed of progression of the surface low from its first point of observation (at 12z 16th Dec., south of Iceland) it can be deduced that this structure is associated with the instability in the model that will develop into the low 48 hours later. There is also a minimum bredmode structure off the coast of Newfoundland. At this time and location, the entire region occupied by the discussed bredmode activity also displays large and extensive analysis increments.

The effect on UM performance of this situation may be assessed by a comparison of the two Control and EBS forecast difference fields shown in the figure for T+72. The EotD forecast from 12z 14th December has reduced the forecast error relative to the control forecast by approximately 7mb at its maximum, and has had the effect therefore of reducing the amount of over-deepening produced by the control forecast. The EotD forecast is also marginally better in position, with the low forecast correctly to be further to the south east (this is not obvious from the forecast differences shown in the figure, but is evident from a comparison of mslp fields, not shown).

At 12z 15th December the bredmode structure over Greenland has moved out over the north Atlantic (left column, middle), whilst the one to the south has moved westwards over Newfoundland. The degree of analysis increments in the north Atlantic region is now vastly reduced, although there is still a degree of increment present in the vicinity of the bredmode to the north. This is therefore an indication that the model has an improved representation of the developing cyclone (background field close to observations), and is presumably the reason for the sudden increase in forecast accuracy shown in the T+48 figure. However, the bredmode associated with the system still has an effect on the forecast, the impact of which may be observed along the middle column of the figure, verified at the same time as earlier (12z 17/12). Although the control forecast at the T+48 range is now greatly improved, the EotD still shows a small degree of improvement, with a reduction in the over-deepening of approximately 5mb.

At 12z 16th December (left column, bottom) the bredmode structure to the north is consistent in location with the first observation of the low pressure system, although its maximum is slightly further north due to the presence of a further cyclone in this position. The VAR analysis increments are still indicative of a developing cyclone and are now considerably more organised than previously (indicating that the model has a better representation of the development at this time than at two days previously). A comparison of the T+24 difference plots shows very little difference between the VAR and EotD assimilation runs.

This experiment confirms once again that given a suitable bredmode structure, the EBS will facilitate a change to the analysis increments in order to better represent the observations in the region, and this results (in this case) in two improved medium range forecasts (T+72 and T+48 both show significant signs of EotD impact). When there is both bredmode and VAR activity (shown by the correlation between the bredmode to the north and analysis increments occupying the same area on the 15th and 16th Dec) and the forecast is relatively good, the EBS is shown to have no detrimental effect on the forecast, even though the EBS will be active in modifying the VAR analysis at this time.

This case study is also a good illustration of how bredmode activity can be used to give useful information about developing regions of the model atmosphere. The instability that eventually developed into a cyclone over Iceland was associated with a bredmode that existed long before the first indications in the mslp fields (identified here over Greenland but could be tracked back further). By their nature, all bredmodes will be associated with baroclinic zones and cyclonic storms as these features will develop rapidly in the model from analysis to analysis.

EotD output could therefore be used by forecasters as additional information on developing regions of the atmosphere and where particular attention should be focussed on whether meteorological features within these regions are likely to be well forecast or not. Very large bredmode structures tend to be more indicative of poor analyses because the bredmode originates from structures changing rapidly in position and magnitude from one poor analysis to the next.

However, bredmodes become more focussed around meteorological features as the analysis improves because the origin of the bredmode is now more a result of changes within the atmospheric states of a developing front or a deepening low.

An example of this is shown in **Figure 17**, in which at 12z 14th December the bredmode structure over Greenland is large and diffuse. As the days progress, and the analysis improves the structure becomes deeper and more focussed around the area of the developing low pressure system.

5. Discussion & Recommendations

The GCT and EotD systems behave as intended in their role of modifying the way in which VAR assimilates observational data. The GCT acts to incorporate flow dependence in VAR, whilst the EotD system acts to vary the influence of observational data depending on the inferred background error.

Both systems show good meteorological behaviour.

In pseudo single observation tests, the GCT responds in the vicinity of baroclinic zones by producing an increment distribution for the analysis that resembles the observation 'flowing' up the frontal zone. The EotD also exhibits a response to frontal zones – identifying them by developing bredmodes in their location, and maintaining their structure in the model by producing bredmodes that also appear to 'flow' up the temperature gradient. The impact of the GCT on operational analysis increments is observed to be consistent with those of the single observation tests. Its effect on UM analyses is measurable and is observed to be greatest within the northern and southern hemisphere storm tracks. This is consistent with the theory behind the GCT in that its maximum effect should be in the locale of fronts, jets and cyclones.

The GCT's effect on frontal zones was investigated in detail, with cross sections taken through regions of maximum modification in the analysis (not discussed in this report). Although measurable, this analysis showed that only minor modifications (slight adjustments of position or gradient) had been performed by the GCT on the baroclinic structure.

The impact of the GCT on storm track forecast accuracy is observed to be relatively small in case studies. However, small positive changes were observed in forecast mslp accuracy ranging out to T+72. This result is not surprising when taken into context with the minor changes observed to frontal zones by the GCT within the context of the Global Model.

Evidence in these case studies suggest that the GCT may have a significant effect on precipitation rates. Further investigation of this effect is intended to be carried out in future trials.

The impact of the EotD on operational analysis increments is also observed to be consistent with those of the single observation tests, and its effect on UM analyses is also greatest within the northern and southern hemisphere storm tracks. Impact location is consistent with the design of the EotD in that they should identify regions of rapidly growing or decaying model states, and these are concentrated within the jet and frontal regions. The effect of the bredmodes used in the EotD on the VAR analyses was investigated in detail. In all cases it was observed that the bredmode information was having the designed effect, with observational information being distributed in response to the surrounding bredmode activity. The changes in analysis increments could be directly attributed to the observed improved 3 day forecast.

The EotD is observed to have a more consistent impact on storm track and depth forecast accuracy than the GCT. In two 3 day forecast cases documented in this report, a combined position and deepening 30hPa error was reduced by approximately 7hPa in one case, and in the other case a 5hPa deepening error was reduced to a 2hPa error with a separate improvement in position. However, it is incorrect to deduce from this that EotD always produces improved forecasts. In many cases no observable or minor effects are seen in the forecasts. EotD is still dependent on the available observations and so even if bredmode activity is large in some area, observational information must still be within those bredmode regions for an effect on the analysis to be seen. Even if observational information and

bredmode activity do coincide there is still not a one to one correspondence between this and improved forecasts.

The EotD has been observed to be a relatively successful initiative in this study. The EBS is seen to generate bredmodes that identify areas of rapidly changing states which are meteorologically as one would anticipate. These bredmodes are observed to modify the VAR distribution of observational information both in a meteorologically sound way and in a way which is consistent with the intent of EotD. Investigations have shown that operational observational data is distributed correctly in response to the bredmode field. Extensive modifications to the VAR analysis field are observed which, based on the cases studied during these trials, lead to either neutral or improved forecasts. No significant detrimental effect to a forecast has been observed during these trials.

The differences in the results of the two schemes may not be too surprising however, if one considers the way in which each scheme is designed to work. Consider the hypothetical situation shown in Figure 18 which schematically represents situations in which the model background is good and poor. A reliable observation in this scenario has detected a temperature which is appropriate to the warm side of the frontal zone in the model.

In situation (a), the 'warm' observation is on the wrong side of the front according to the model background. In this situation, the GCT will have no impact on VAR to correct the forecast as it is not within the immediate vicinity of the frontal zone. This report has shown that frontal zones are associated with bredmode structures however, and it is logical to assume that incorrectly analysed frontal structures would change rapidly in position from time step to time step. This region is therefore likely to be in an area of large bredmode activity. In this scenario therefore, one would expect the EotD to have some impact in correcting the position of the frontal zone.

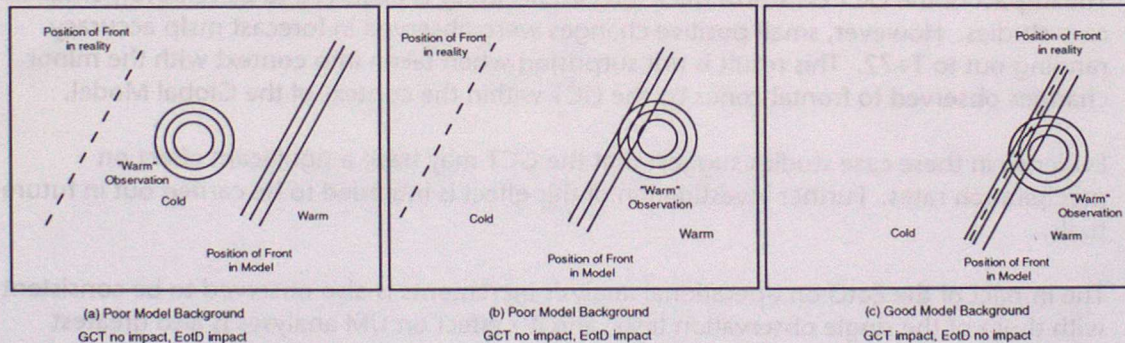


Figure 18 Hypothetical situation involving a 'good' observation and a frontal zone. (a) and (b) represents a Poor Model Background, and (c) represents a good model background field.

Situation (b) is the same situation as (a) but here the observation is on the 'correct' side of the model frontal zone in the 'warm' air. Here the GCT will still not correct the frontal zone positional error, and indeed may even strengthen the zone relative to VAR, as the observation will respect the baroclinicity within this region of the model. Again however, the bredmode activity would be large in this area and the EotD may have an impact in correcting the position of the front.

Situation (c) is a good Model representation of the atmosphere, with the frontal zone in the correct place. Here, the GCT is active and the frontal zone is strengthened relative to VAR. Perhaps a better representation of precipitation rates may result from the activity of the GCT in this way. The area would still be occupied by a bredmode however (probably of smaller extent to scenarios (a) and (b) as these states are not as likely to have changed as much, being of good representation) and so some small impact of the EotD may be expected as EotD shows better flow dependence around frontal zones than VAR. In these hypothetical situations it is clear that the GCT can only improve an already good analysis, whereas the EotD is more active in cases of poor analyses.

This process may be taking place in the GCT case studies of Section 3.2.1. It was shown here that cyclone C had the smallest differences of the θ_1 analysis when compared with cyclones A and B. From this, one expected that Cyclone C would be the least likely to exhibit positive (or negative) impacts in the forecast performance. However, Section 3.2.2 showed that the forecast of cyclone C exhibits a small positive impact on the central surface pressure, and a significant impact on the precipitation rate.

It was discussed in Section 3.2.2 that Cyclone B was poorly forecast in the Control Trial and that the GCT failed to significantly improve the situation. It was also shown that Cyclone C was relatively well forecast, but that the GCT did show some improvement in this case to both the central pressure and precipitation fields. Figure 19 shows the pstar bredmode structures for 12z 12/12/99, with contours showing the mean sea level pressure field at that time. Cyclone A is associated with a very large intense bredmode structure, whilst cyclone B also occupies a region of significant bredmode activity. Cyclone C, however, occupies a region with the least bredmode activity.

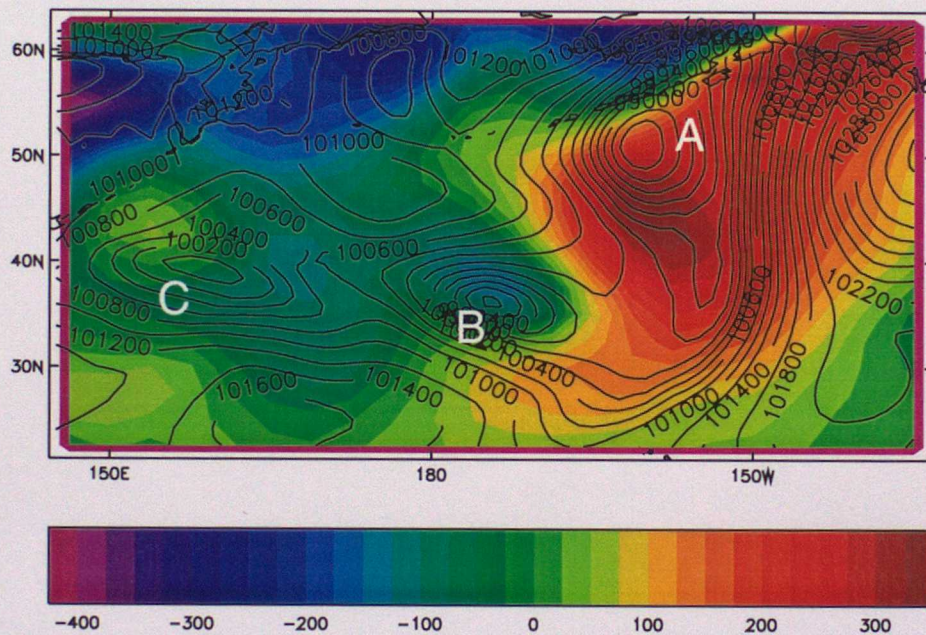


Figure 19 Pstar Bredmode Structure (colour field) and mean sea level pressure (contours). Labels A, B and C refer to cyclones discussed in Section 3.2. Cyclone C is associated with the least bredmode activity.

It has been discussed in this report that the relative degree of bredmode activity is correlated with the probable accuracy of the background state at that time. Cyclones A and B are therefore likely to be associated with poorer forecasts than cyclone C. From the hypothetical situation outlined above, one would therefore expect little impact of the GCT in cyclones A and B, but a more significant impact in cyclone C.

This is consistent with the findings of this report, and perhaps shows that both schemes are operating within their design criteria.

In this study of EotD, it was decided that it would be beneficial to assess its performance as the system stood when designed and implemented, with the knowledge that much work had gone into setting the system up with various parameters. This provides a good baseline from which to measure EotD performance. However, the coding of the EotD system involves the 'alpha' control variable which effectively incorporates the bredmode structures into the assimilation procedure. The degree of impact of the bredmode on 3D VAR is controlled by two parameters which control the structural and temporal extent of alpha. The alpha parameters may therefore preferentially select convective processes or baroclinic zones,

6. Acknowledgements

The EotD coding and development was performed by Dale Barker. GCT coding and development was performed by Mark Dubal. The EotD trial used in this study was performed by John Bray. The GCT trial used in this study was performed by Sean Swarbrick.

The Author is indebted to Sean Swarbrick for providing the training required to run SCS trials, VAR tests, assessment of the verification suite, physical explanations regarding the Geostrophic co-ordinate transform and a menagerie of VAR/UM/GCT/EBS/SCS/IAU/COSMOS system problems.